

The Ionospheric Effects Symposium 2023

Abstract Book



IES 2023



IES 2023

Global Responses of Equatorial/Low-Latitude Ionosphere to CME-driven and CIR-driven Geomagnetic Storms

Akala, Andrew University of Lagos

Yuichi Otsuka, Institute for Space-Earth Environment, Nagoya University, Nagoya, Aichi, Japan

Oluwole Johnson Oyedokun, Department of Physics, University of Lagos, Akoka, Lagos, Nigeria

Jonathan Umunna, Department of Physics, Federal University Ndufu Alike, Ebonyi State, Nigeria

Geomagnetic storms are global disturbances in the Earth's magnetic field caused by a conglomeration of solar and interplanetary events, and they are capable of modulating the Earth's ionosphere. Consequently, in this study, we investigated the responses of the global equatorial and low-latitude ionosphere to two Coronal Mass Ejection (CME)-driven geomagnetic storms of 17 March 2013 and 17 March 2015, and another set of two Co-Rotation Interaction Region (CIR)-driven geomagnetic storms of 1 June 2013 and 7 October 2015. We used equatorial and low-latitude TEC data obtained from seventeen GPS stations, and five magnetometer stations in five longitudinal sectors; namely, Pacific West, South American, African East, Indian Ocean/Asian, and Pacific East sectors. GUVI satellite data were used to determine storm-time changes in thermospheric composition. Prompt Penetration Electric Field (PPEF) derived from the magnetic field data in conjunction with the University of Colorado model data were characterized alongside the four geomagnetic storms. CME-driven storms recorded higher ionospheric geoeffectiveness than CIR-driven storms. Geomagnetic storms' geoeffectiveness followed semi-annual periodicity, highest in the March equinox and least in the June solstice. Aside from the seasonal effect, the local time of the storm's onset dictates ionospheric responses to geomagnetic storms. High occurrences of quiet-time irregularities were observed in March 2013 and March 2015 and significantly higher in the South African sector which we attributed to the weak geomagnetic field configuration in the sector.

Space Weather Applications & Services, Storm Effects, Equatorial Dynamics & Drivers, Equatorial Irregularities

Storm-time hourly morphologies of the Equatorial Ionization Anomaly (EIA) crests and their extended features along 110-125°E meridian

Akala, Andrew University of Lagos

Ayangbemi, John A., Department of Physics, University of Lagos, Nigeria

Otsuka, Yuichi, Institute for Space-Earth Environment, Nagoya University, Nagoya, Aichi, Japan

This study investigates storm-time hourly morphologies of the Equatorial Ionization Anomaly (EIA) crests and their extended features along the Asian/Australian meridian lines. We used TEC derived from the observation data obtained from GPS receivers lined at $\sim\pm 75^\circ$ latitude along 110-125°E meridian. Four geomagnetic storms of 2013 and 2015 St. Patrick's Days, 1 June 2013, and 7 October 2015 were studied. The quiet days of the month of each storm occurrence was used as reference to evaluate storm-time responses of the EIA-TEC to geomagnetic storms. There were clear hemispheric asymmetries in plasma distributions. At 0000–0500 LT, plasma was localized around the magnetic equator with a single peak for each hour. At 0600–1100 LT, bifurcation of the EIA peak gradually commenced, with both peaks tilted to the northern hemisphere but the southern crest recorded higher magnitude of TEC. At 1200–1700 LT, the EIA was well-formed, particularly from 1400–1700 LT and the magnitude of the southern crest was higher than that of the northern crest, but conversely at 1200 and 1300 LT. At 1800–2300 LT, there was a reversal; the magnitude of the northern crest was higher than that of the southern crest, and plasma was localized around the magnetic equator with a single peak at 2300 LT. We also observed secondary minor peaks at $\sim\pm 45^\circ$ magnetic latitudes. The daily metamorphosis of the EIA structures followed the same morphologies during quiet-time and storm-time, except for the storm effect on the EIA crests in terms of: expansion/increase in TEC or decay/decrease in TEC as may be dictated by whether the minimum main phase of a storm occurred at daytime or at nighttime.

Space Weather Applications & Services, Storm Effects, Equatorial Dynamics & Drivers, Equatorial Irregularities, High Latitude Structure & Irregularities

Sporadic-E and GNSS Scintillation

Beach, Theodore Institute for Scientific Research, Boston College, Chestnut Hill MA, USA

Multiple recent reports have claimed observations of daytime L1 band (1.6 GHz) amplitude scintillation associated with sporadic-E from ground-based GNSS measurements. While there is a long history of detecting ground-based VHF scintillation associated with sporadic-E, if the L1 observations hold up it could say something new about ionospheric structure. Refractive index fluctuations in the ionosphere decrease as $1/f^2$ so the phase impacts are about 2% as strong at L1 as at 250 MHz for the same electron density structure. Moreover, L1 measurements respond to smaller irregularity length scales transverse to the line of sight and the spectral density function (SDF) of irregularities typically decreases with decreasing scale size. The E-region is a thin layer, so there is not large distance to integrate through to increase the phase effects. For comparison, some of the strongest historical 250 MHz VHF scintillation observed to be associated with sporadic-E layers had an amplitude scintillation index, S4, of 0.4–0.6. Using frequency scaling for power-law spectral indices appropriate to E-layer instabilities, this translates to an L1 S4 of 0.02–0.04, which is typically at or below the S4 noise floor for GNSS receivers. Slant-path enhancements could raise this to 0.09 at low elevations. Alternatively, could coherent structures, such as discrete edge-diffraction mechanisms, plausibly generate observable S4 levels at L1? This talk will explore both random and coherent scintillation mechanisms to assess the physical conditions required to generate an S4 of 0.2 or higher at 1.6 GHz due to E-region irregularities. In particular, are the required electron density fluctuations consistent with what is physically likely for sporadic-E?

Scintillation & Propagation Effects on GNSS and Other Systems

Using the Ionosphere to Amplify Whistlers and EMIC Waves from Ground Transmitters for Reduction of Radiation Belt Particle Populations

Bernhardt, Paul (Univ. of Alaska Fairbanks, Fairbanks, AK)

Hua, Man (UCLA, Atmospheric and Oceanic Sciences, Los Angeles, CA)

Bortnik, Jacob (UCLA, Atmospheric and Oceanic Sciences, Los Angeles, CA)

Ma, Qianli (Boston University, Boston, MA)

Harid, Vijay (University of Colorado Denver, Denver, CO)

Golkowski, Mark (University of Colorado Denver, Denver, CO)

Howarth, Andrew (University of Calgary, Calgary, AB, Canada)

The concept of this research is that radiation belt fluxes responsible for damage of satellites are rapidly reduced using scatter by intense whistlers from Rocket Exhaust Driven Amplification (REDA) of VLF in the Ionosphere. Both natural and manmade populations of energetic trapped radiation in the magnetosphere can have major impacts on space objects. A new technique has been developed to remove these “killer electrons”. Whistler-mode, VLF waves can scatter trapped energetic electrons into low pitch angle orbits resulting in enhanced particle precipitation and loss in the lower atmosphere. This energetic electron loss process is greatly enhanced by intentional amplification of whistler waves in the ionosphere with a Whistler Traveling Wave Parametric Amplifier (WTWPA). Large amplitude (1000 pT) whistlers generated by intentional amplification of existing VLF waves are sufficient for regional depletion the energetic particle population in the radiation belts. The scattering into the atmospheric loss cone requires only few minutes rather than the multi-day periods it would take naturally. Ground-based VLF transmitters located around the world generate signals that leak through the bottom side of the ionosphere in the form of whistler mode waves. Such parametric amplification is driven by a Lower Hybrid (LH) wave pump that may be generated (1) by pickup ions from orbiting rocket motor burns or (2) with high power HF facilities such as HAARP in Alaska. Satellite measurements of WTWPA, using intense LH-pump oscillations found in spacecraft exhaust plumes, have shown between 30- and 50-dB intensification of whistler waves in space. The scattering of radiation-belt, energetic particles by amplified whistlers employs either the UCLA quasi-linear Fokker Planck model (QLFP) or the UCD Vlasov-Maxwell (V-M) model to compute the fluxes of precipitating electrons [Bernhardt et al., 2022]. The quasi-linear and non-linear wave-particle interaction approaches can describe the impacts the intensified whistlers on the space weather environment including regionally enhanced D-region densities.

Bernhardt, P. A., Bougas, W. C., Griffin, M. K., Watson, C., Langley, R. B., Howarth, A. D., et al. (2021). Strong amplification of ELF/VLF signals in space using neutral gas injections from a satellite rocket engine. *Radio Science*, 56, e2020RS007207.

Bernhardt, P.A., (2021) The Whistler Traveling Wave Parametric Amplifier (WTWPA) Driven by an Ion Ring-Beam Distribution from a Neutral Gas Injection in Space Plasmas, IEEE Transactions on Plasma Science. 49, 6, 1983-1996.

Hua, M., Bortnik, J., Ma, Q., & Bernhardt, P. A. (2022). Radiation belt electron acceleration driven by Very-Low-Frequency transmitter waves in near-Earth space. Geophysical Research Letters, 49, e2022GL099258.

Bernhardt, P. A., Hua, M., Bortnik, J., Ma, Q., Verronen, P. T., McCarthy, M. P., et al. (2022). Active precipitation of radiation belt electrons using rocket exhaust driven amplification (REDA) of man-made whistlers. Journal of Geophysical Research: Space Physics, 127, e2022JA030358."

Space Weather Applications & Services, Active Experiments

Finding Space Debris with Orbit Driven Plasma Waves in the Ionosphere

Bernhardt, Paul (Geophysical Institute Univ. of Alaska, Fairbanks, AK, USA)

Scott, Lauchie (DRDC Ottawa Research Centre, Ottawa, Canada)

Howarth, Andrew (Phys. Dept. University of Calgary, Calgary, Canada)

The concept of this research is that ionospheric plasma waves generated by space debris could be detected to help space agencies protect spacecraft from collisional damage. Research scientists in the United States and Canada have demonstrated a new way to locate pieces of space debris that threaten spacecraft and satellites in orbit. Space debris, or space junk, consists of leftovers from human-made objects – such as discarded launch vehicles or parts of a spacecraft – typically trapped in orbit around the Earth. Currently, NASA tracks over 27,000 such objects in low Earth orbit. The European Space Agency (ESA) estimates that the total mass of all space debris in Earth's orbit is close to 22 million pounds (10 million kilograms). The number of debris that are too small to be tracked, yet large enough to cause severe damage upon impact, is in the millions. Since both space debris and active spacecraft travel at tremendous speeds of about 25,000 kilometers per hour, an impact of even a tiny piece of orbital debris with a spacecraft could create significant issues.

Traditionally, space debris are detected with satellite and ground sensors that use optics and ranging radars. These methods, however, cannot detect many smaller debris. Scientists from the University of Alaska and the University of Calgary have demonstrated a novel technique for locating space debris by measuring the electric fields that surround them while in motion through the plasma in the ionosphere. This new technique, called Space Object identification by in situ Measurements of Orbit-Driven Waves (SOIMOW), relies on creation of plasma oscillations as charged space debris move through space.

The Earth is surrounded by the ionosphere – a plasma layer with thermal ions and electrons. All satellites move through this plasma at speeds greater than the speed of sound. Both spacecraft and space debris become electrically charged as they are bombarded by solar photons and electrons from the plasma environment. Hypersonic charged objects can stimulate a wide range of plasma waves as they travel through the ionosphere, crossing the Earth's magnetic field lines.

The Radio Receiver Instrument (RRI) on the Canadian SWARM-E satellite has been attempting to detect plasma waves around orbital debris using direct measurements at a point of interest. The RRI observations seem to show magnetohydrodynamic (MHD) waves and electrostatic waves as far as 90 km away from the space object producing them. MHD waves are produced by “striking” magnetic field lines, much like plucking a guitar string. Electrostatic waves are disturbances in the plasma that are caused by oscillating charged particles. The peak of this enhanced signal is found at the closest approach between the RRI detector and the target object. The cloud of enhanced plasma-wave noise lasts for about 20 seconds and is interpreted as spacecraft-driven turbulence comprised of a mixture of different kinds of plasma waves.

The challenge is to convert these newly discovered waves into EM modes that propagate long distances to be recorded by remote satellites or even on the Earth. Accurate determination of source locations would use the angular spread and time of arrival recorded from multiple

receivers. Processed data may yield an image of the space debris traveling across the radio sky. The SOIMOW team is conducting experiments to determine if stimulated scatter from the UAF HAARP high power, ground-based transmitter can be employed to observe the trajectories of satellites and space debris.

P.A. Bernhardt, L. Scott, A. Howarth, G. J. Morales, Space Object Identification by Measurements of Orbit-Driven Waves (SOIMOW), Submitted to Physics of Plasmas, 2023.

Space Debris Monitoring and Remediation

Detection of Spread-F, foF2 values and Planetary and Gravity Wave Signatures using Digisonde instruments and their comparison with COSMIC-1/FORMOSAT-3, SAMI and IRI data

Bhaneja, Preeti USRA/NASA-GSFC

Bullett, Terry; CIRES/NCEI/NOAA

Klenzing, Jeff; NASA-GSFC

A comprehensive statistical study of Spread F using digisonde data from low and midlatitude global sites has been conducted. Data from five midlatitude stations in the north-American include: Ramey AFB, Puerto Rico (18.5°N, 67.1°W, -14° declination angle) for 1996-2011, Wallops Island, Virginia (37.95°N, 75.5°W, -11° declination angle) for 1996-2011, Dyess, Texas (32.4°N, 99.8°W, 6.9° decl. angle) for 1996-2009, Boulder, Colorado (40°N, 105.3°W, 10° decl. angle) for 2004-2011, and Vandenberg AFB, California (34.8°N, 120.5°W, 13° decl. angle) for 1996-2009. Low-latitude stations include: Ascension Island (7.9°S, 14.4°W, -15.09° decl. angle) from 2000-2014, Kwajalein (8.71°N, 167.7°E, 7.5° decl. angle) from 2004-2012. Multiple algorithms have been written to process the raw data and determine spread F by using edge detection and pattern recognition techniques. Pattern recognition algorithms are used to determine the presence of both range and frequency spread F. Algorithms have also been written to find foF2 and hmF2 values for obtaining the density profile of the ionosphere. Findings based on work carried out to date include:

- Determination of seasonal and solar cycle variation patterns.
- Correlation between digisonde, COSMIC-1/FORMOSAT-3 satellite data and SAMI and IRI models values to check for validity of data.
- Wave analysis has been performed to detect the presence of planetary and gravity wave patterns in foF2 values with periods ranging from a few hours to a few days and for various seasons.

Equatorial Irregularities, Midlatitude spread F, Digisonde data analysis

HF scattering of ocean waves using HAARP

Briczinski, Stanley Naval Research Lab

Coombs, Joseph NRL

Siefring, Carl NRL

Bernhardt, Paul University of Alaska Fairbanks

Sletten, Mark NRL

McCarrick, Mike, University of Alaska Fairbanks

McCarrick, Mike University of Alaska Fairbanks

Howarth, Andrew University of Calgary

James, H. Gordon University of Calgary

HF radar scattering is ideally suited for remotely measuring the ocean wave spectrum because electromagnetic wavelengths in the HF band scatter resonantly with ocean waves typically near the spectral peak. In addition, HF transmissions can illuminate broad sections (1000s of km) of the ocean's surface, providing information not possible with other techniques. Bernhardt et al. [2016] recently demonstrated detection and analysis of HF signals scattered off the ocean surface from an Over The Horizon Radar (OTHR) system that were received by the ePOP Radio Receiver Instrument (RRI) on the Swarm-E satellite. Scattered power obtained at multiple points in the satellite orbit can be used to determine a slice through the ocean wave height spectrum using imaging techniques, including those for synthetic aperture radar (SAR), followed by an inversion based on established ocean scattering theory.

We present data obtained using the High-Frequency Active Auroral Research Program (HAARP) operating in modes similar to OTHRs. The HAARP facility has unique advantages over lower-latitude measurements. HAARP's polar location allows HF rays to be reflected by both sea ice and ocean waves (as well as the boundary between these domains). Of particular interest is the possibility to remotely mapping sea ice locations. A new technique using coded pulses was first utilized during experiments conducted in Spring of 2022. The new technique was used in an attempt to improve range and Doppler resolution for HF ocean wave scattering collected by the Swarm-E satellite. The new technique also eliminates the need for HF facilities to transmit perfectly linear FMCW chirped waveforms. We present comparisons of our new technique to that of the previous chirped pulse method.

Naval Research Laboratory efforts in this research is funded by the NRL 6.1 Base Program.

P. A. Bernhardt et al., ""Large area sea mapping with Ground-Ionosphere-Ocean-Space (GIOS),"" OCEANS 2016 MTS/IEEE Monterey, 2016, pp. 1-10, doi: 10.1109/OCEANS.2016.7761503."

Active Experiments

The Variable Voltage Ion Protection Experiment (VVIPRE): Thermospheric and Ionospheric Remote Sensing from the ISS

Budzien, Scott Naval Research Laboratory

Dymond, Kenneth (NRL)

Fritz, Bruce (NRL)

Nicholas, Andrew (NRL)

Stephan, Andrew (NRL)

Wagner, Ellen (NRL)

VVIPRE is a demonstration space experiment built by the U.S. Naval Research Laboratory to show how low-cost variable voltage power supplies can protect sensitive spaceflight detectors from space plasma ion damage, extend sensor lifetimes, and deliver high-quality measurements of the Earth's upper atmosphere. Spacecraft charging and ambient ion impingement can cause noise, detector damage, and reduced sensor lifetime on-orbit. The variable voltage power supplies compensate for variations in spacecraft potential to reduce or eliminate this unwanted ion flow. Then naturally-occurring ultraviolet airglow can be measured to specify the atmosphere globally. VVIPRE will demonstrate successful ion mitigation by delivering space environment remote sensing data suitable for DoD model use. VVIPRE combined with the ECLIPSE experiment forms a powerful atmospheric observatory on the ISS.

Optical Remote Sensing

Large Scale Traveling Ionospheric Disturbances in the Topside Ionosphere

Burrell, Angeline G NRL

Dhadly, Manbharat Dhadly, (NRL)

Zawdie, Katherine (NRL)

Sassi, Fabrizio (NASA-GSFC)

Understanding the formation, progression, and global impact of Large Scale Traveling Atmospheric/Ionospheric Disturbances (LSTADs/LSTIDs) is a long-standing challenge in global space weather research. This has been a particularly perplexing problem due to the strongly coupled nature of the high-latitude ionosphere-thermosphere (I-T) system, where they are believed to originate from. At high latitudes, the magnetosphere dumps a large amount of energy (both directly and indirectly) into the I-T system through Joule heating, auroral particle heating, and ion drag. LSTADs are a commonly observed thermospheric response to magnetospheric energy entering the I-T system. It is believed that LSTADs drive a similar wave response in the ionosphere, known as LSTIDs. Recent studies suggest that LSTADs/LSTIDs may also play an important role in transporting high-latitude variability to lower latitudes.

This study examines the impact of LSTIDs propagating from higher latitudes on the topside equatorial ionosphere. The altitude variation of LSTIDs is investigated using a combination of observational and modeling methods. The geomagnetic storms that occurred on the 25-26 March 2014 are used as a case study, as several Low Earth Orbit (LEO) satellites with orbits at different altitudes in the topside ionosphere were operational. The variations seen in the observations are then explored using model runs, which further allow a more detailed analysis of altitude variations once their variations are validated against the observational data.

HF Modeling, TIDs and Geolocation, Topside & Plasmasphere

A Limb-to-disk Algorithm for Mapping Scintillation Observations Along Radio Occultation Ray-paths to the Vertical Propagation Geometry

*Carrano, Charles*¹, Keith Groves¹, William McNeil¹, Endawoke Yizengaw², Paul Straus², Ron Caton³, and Dallin Smith³

¹Boston College Institute for Scientific Research, ²Aerospace Corporation

³Air Force Research Laboratory

Modern radio occultation (RO) receivers such as the TGRS instrument onboard the COSMIC-2 satellites can routinely provide high-rate observations during ionospheric scintillation. TGRS, for example, provides 50 Hz and 100 Hz samples of amplitude and phase for GPS and GLONASS transmissions, respectively, whenever an elevated S4 triggers downlink of the occultation. The high-rate data enables direct measurement of the amplitude and phase scintillation indices (S4 and sigma-phi) as well as indirect (model-inferred) estimation of turbulence strength integrated along horizontal radio-occultation ray-paths. While useful, a ground-based user of satellite radio services (for communications, navigation, radar, etc.) would generally prefer to know the scintillation indices along a space-to-ground propagation path, possibly at a different operating frequency than TGRS uses to remote sense the ionosphere.

This paper presents a new limb-to-disk (L2D) algorithm for mapping scintillation along radio occultation ray-paths from the horizontal to the vertical propagation geometry. Since both turbulence strength and propagation distance contribute to the measured RO S4, it is necessary to first locate the irregularity region before the horizontal to vertical mapping is performed. The L2D algorithm accepts, as input, bubble geolocations from the Boston College TGRS Geolocation product, which was developed and validated under the COSMIC-2 calibration/validation program (and the results were presented at the 2022 Beacon Satellite Symposium). The challenge with L2D mapping is that a radio occultation does not provide information about the state of the plasma above or below the horizontal ray-paths, whereas a vertical propagation path is sensitive to irregularities at all altitudes within the vertical channel. Therefore, the altitude distribution of plasma turbulence must be modeled. We assume that $\Delta N/N$ is independent of altitude inside a bubble, and we justify this assumption by comparing density profiles obtained from Abel inversion and IRI with vertical profiles of turbulence strength inferred from a special class of occultations. These special occultations provide multiple geolocations at various altitudes within the same plasma bubble, thereby allowing vertical profiles of turbulence strength to be measured.

Our comprehensive model for limb-to-disk translation accounts for the transmit (TX) and receive (RX) frequencies, TX/RX platform velocities and propagation direction with respect to the geomagnetic field, and the stochastic properties of the irregularities (spectral index and anisotropy). We validate L2D predictions of S4 using ground-based GNSS scintillation data collected in multiple longitude sectors during a wide range of solar flux conditions. Vertically integrated turbulence strength estimates from the L2D algorithm are being produced in near real-time at Boston College and are being ingested in the RF Ionospheric Scintillation Analysis (RISA) tool. The goal of RISA is to provide global specification of the ionospheric scintillation environment using on-demand data-driven projections (“nowcasts”) and climatology.

The views expressed are those of the authors and do not reflect the official guidance or position of the United States Government, the Department of Defense or of the United States Air Force.

Approved for public release; distribution is unlimited.

Radio Occultations & Tomography

An Improved Starting Field for Full Wave Modeling of High-Frequency Propagation in the Ionosphere

Carrano, Charles S.¹, Charles L. Rino¹, Louis Fishman²

¹Boston College

²Tulane University

In a recent paper at the 2022 Beacon Satellite Symposium, we demonstrated that split-step Fourier methods, commonly implemented via the multiple phase screen technique, are unable to accommodate the large bending angles that occur when high-frequency (HF) waves propagate in the ionosphere. Alternative approaches that can accommodate these large bending angles include the split-step Padé method (Collins, JASM, 1989), a high-frequency operator symbol construction derived from phase space path integral methods (Fishman & McCoy, ASA, 1987), and a uniform high frequency operator symbol construction that is extremely accurate over a substantial parameter space (Fishman et al., WM, 1997). Each of these techniques require a starting field to initiate the computation. For a ground-based antenna that transmits a confined beam into the free-space region below the ionosphere, there is no difficulty initializing the computation if the beam radiates no appreciable energy at ionospheric altitudes as it enters the computational grid. However, in most HF applications the transmit pattern is broad and energy radiates essentially in all directions. In that event, a starting field that accommodates both the boundary conditions and the interaction with the ionosphere is required to initialize the computation. In the computational acoustics community, the PE self-starter proposed by Collins is widely used for this purpose (Collins, ASA, 1992; Collins, ASA, 1999). When applied to ionospheric problems, however, the PE self-starter does not properly model the scatter of energy by the extremely large propagation angles needed to reach the ionospheric region directly above the source. Orienting the reference direction toward the zenith could potentially mitigate this problem, but at the expense of increasing the range-dependence of media variations (which would increase the overall computational effort). For near vertical incidence skywave (NVIS) propagation problems, where one is interested in both vertical and downrange propagation effects, a more flexible and robust approach for generating a starting field is needed.

In this paper, we consider an alternative starting field for full wave modeling of high-frequency propagation in the ionosphere, based on the uniform asymptotic expansion of the generalized Bremmer series (de Hoop and Gaultesen, JAM, 2000). The generalized Bremmer series may be viewed as a full-wave extension of the high-frequency geometrical ray series representation of the wave field. It can accommodate extremely large propagation angles and, indeed, it includes the evanescent modes which the PE self-starter intentionally suppresses (for increased numerical stability). The de Hoop and Gaultesen formalism provides a uniform high-frequency (UHF) approximation to the infinitesimal Green's function in closed (analytic) form, expressed in terms of the ionospheric refractive index and its first two derivatives. We show that a hybrid algorithm consisting of the UHF Green's function starter field near the source, followed by PE split step marching downrange, can produce accurate fields everywhere in space for NVIS propagation problems at HF frequencies exceeding the plasma frequency. Since this marching algorithm provides a problem-specific (numerical) Green's function everywhere in space, more complex transmit antenna patterns may be modeled via linear superposition. We benchmark the code

using an exact representation of the Green's function for an Epstein (sech squared) ionospheric profile and perfectly conducting boundary conditions implemented via the method of images.

HF Modeling, TIDs and Geolocation

Modeling the Day-to-Day Variability of Midnight Equatorial Plasma Bubbles with SAMI3/WACCM-X

Chou, Min-Yang *NASA GSFC, CCMC*

Yue, Jia (NASA GSFC)

Sassi, Fabrizio (NRL)

Huba, Joseph (Syntek Technologies)

McDonald, Sarah (NRL)

Tate, Jennifer (Computational Physics, Inc)

Pedatella, Nicholas (NCAR)

Randall, Cora (CU Boulder)

Harvey, Lynn (CU Boulder)

It is well-known that equatorial plasma bubbles (EPBs) are highly correlated to the post-sunset rise of the ionosphere on a climatological basis. However, when proceeding to the daily EPB development, what controls the day-to-day/longitudinal variability of EPBs remains a puzzle. In this study, we investigate the underlying physics responsible for the day-to-day/longitudinal variability of EPBs using the Sami3 is A Model of the Ionosphere (SAMI3) and the Whole Atmosphere Community Climate Model with thermosphere-ionosphere eXtension (WACCM-X). Simulation results on October 20, 22, and 24, 2020 were presented. SAMI3/WACCM-X self-consistently generated midnight EPBs on October 20 and 24, displaying irregular and regular spatial distributions, respectively. However, EPBs are absent on October 22. We investigate the role of gravity waves on upwelling growth and EPB development and discuss how gravity waves contribute to the distributions of EPBs. Of particular significance is that we found the westward wind associated with solar terminator waves and gravity waves causes midnight vertical drift enhancement and collisional shear instability, which provides conditions favorable for the upwelling growth and EPB development. The converging and diverging winds associated with solar terminator waves and midnight temperature maximum also affect the longitudinal distribution of EPBs. The absence of EPBs on October 22 is related to the weak upward drift induced by weak westward wind associated with solar terminator waves. This study reveals that atmospheric waves can modify the midnight ionospheric electrodynamics, providing conditions identical to the post-sunset ionosphere and favorable for EPB development.

Assimilative and Coupled Models, Equatorial Irregularities

Validating and Improving a Realistic Ionospheric Truth Model for Observing System Simulation Experiments of HF Propagation

Collett, Ian *Orion Space Solutions*

Hughes, Joseph (Orion Space Solutions)

Wilson, Walter "Junk" (Orion Space Solutions)

Crowley, Geoff (Orion Space Solutions)

Colman, Jonah (AFRL)

Landry, Russell (AFRL)

The US Air Force Cover Analysis Program (AFCAP) experiments 1, 2, and 3 have all been multimillion dollar campaigns to perform detailed Observing System Experiments (OSEs) of the ionosphere. Much of that expense has been dedicated to collecting enough observations of the ionosphere to be capable of post processing a “truth” ionosphere that supports additional analysis of alternative OSE experiments. Even after such great expense, significant limitations exist in the regional, seasonal, and decadal breath of available “truth” data. The ability to conduct a quality OSE without having to deploy dozens of sensors and dozens of people to the field would vastly expand the research opportunities across time and location. Such “virtual” OSEs are called Observing System Simulation Experiments (OSSEs) and require a synthetic truth model. For the HF propagation environment relevant to AFCAP, the synthetic truth model must accurately represent small-scale structures that are not present in smooth climatological or physics-based models. These small-scale structures must be physically realistic in both space and time to support OSSEs based on HF propagation. We present a synthetic truth model that attempts to meet these requirements and a path of further development which we believe will achieve this objective.

Our synthetic truth model is constructed from the smooth physics-based Thermosphere Ionosphere Electrodynamics General Circulation Model (TIE-GCM), by incorporating spatial and temporal electron density variations informed by two years of ionosonde measurements at mid-latitudes. The variations present in the ionosonde data that are not resolved by TIE-GCM are stored in terms of vertical, horizontal, and temporal correlations. To produce a realization of the truth model with these realistic electron density variations, the process is to (1) create uncorrelated Gaussian white noise, (2) use a Gaussian kernel in the spatial domain to enforce the vertical and horizontal correlations, (3) transform to the frequency domain to enforce the temporal correlation, and (4) apply this correlated noise to the TIE-GCM parent model.

Recently, using data from AFCAP experiment 2 (AE2), we have performed validation of the truth model’s re of the HF propagation environment. The AE2 data include oblique and vertical incidence soundings with a nominal 15-minute cadence. Ionospheric irregularities manifest as higher frequency variations in the time series of the maximum useable frequency (MUF) of oblique links. For several links of ground distances 500-2000 km, we perform OSSEs (HF raytracing through TIE-GCM and a realization of the truth model) to produce synthetic measurements for comparison. Although the time series observations are not the same because of

the random nature of the truth model, we can compare spectral characteristics of the MUF. While the MUF spectrum for TIE-GCM falls off much quicker than the data, the spectrum for the realistic truth model matches the observed MUF spectra much more closely. Further methods of validation, such as a comparison of the E and F1 layer characteristics between the truth model and AE2 vertical incidence observations, are being pursued.

Improvements to the truth model are being explored. As previously described, the current version of the truth model is created by applying the spatial correlations with a Gaussian kernel and applying the temporal correlation in the frequency domain. We are pursuing an alternative approach using a coupled 4D spectrum of the ionosonde electron density variations that can be enforced in a single consistent step. We have developed numerical code for an N-dimensional Lomb-Scargle Periodogram that can reliably resolve spectral information from a set of non-uniform measurements in both space and time, enabling this kind of approach. In principle, the consistent treatment among the spatial and temporal correlations should allow the truth model to capture phenomena that are coherent in space and time, such as traveling ionospheric disturbances and sporadic E.

HF Propagation & Systems

Over-the-horizon (OTH) Propagation: Ray Trace Model and Measurement Matching

Conroy, James JHU APL

Ellison, Sean (JHU APL)

McFadden, Francesca (JHU APL)

Wiker, Jordan (JHU APL)

Outwater, John (JHU APL)

Predicting the propagation of high frequency (HF) radio wave power from a transmit to a receive location is a critical part of the HF communication system design process. Medium fidelity modeling, such as the work performed by (Francis et al., 2017) and (Cervera et al., 2018) using the Provision of High-frequency Raytracing Laboratory for Propagation (PHaRLAP) toolbox, focused on estimating the signal-to-noise ratio (SNR) of a radar system for a wide range of solar conditions as part of a system design methodology study. Higher fidelity tools also exist such as the High-frequency Channel Impulse Response Function (HiCIRF) (Nickisch et al., 2012), which has been used to perform over-the-horizon radar (OTHR) and communication system modeling. More recently, the ability to predict the power received after one-way propagation was evaluated by several researchers using highly detailed transmit and receive system and ionospheric raytrace modeling, with the results compared to measurement data (Perry et al., 2022; Conroy et al., 2023). In these recent works, it was shown that the ability to predict received power is highly dependent upon three main factors: 1) antenna system modeling, 2) ionospheric channel estimation, and 3) high fidelity raytrace modeling. In particular, the availability of three-dimensional (3D) transmit and receive antenna system models is critical for properly applying gain to propagating ray paths, while the ability to estimate the ionospheric state between a transmit and receive location determines the degree to which raytrace modeling captures the salient propagation effects.

In this paper, we built upon previous modeling and data analysis work, which was expanded to include a full 3D raytrace engine, more detailed antenna simulations, and improved signal detection by way of pulse compression using a transmit signal waveform model. HF data for the study were acquired for 3 days by a software-defined receiver (SDR) at a site in Palm Bay, FL during September, 2022. During the experiments, the CHU and WWV clock timing signals were used to study the effects of the ionosphere on HF propagation, and to anchor our raytrace link budget modeling approach. The quality of the acquired data was initially reviewed to confirm the successful reception of signals, or not, by visual inspection and by listening to the signal playback for the expected messages. Following this quick-look study, we performed a detailed series of SNR calculations, and made note of detections, which were subsequently confirmed by pulse compressing the transmit signal waveform model and data. Detailed transmit and receive antenna patterns were then created and integrated into an oblique propagation model to study the propagation of sky wave modes. For the antenna modeling, the Numerical Electromagnetics Code (NEC) Method of Moments (MOM) simulation was used to generate gain patterns. For the ray trace modeling, the PHaRLAP raytracing toolbox was used to generate sky wave paths using

the International Reference Ionosphere (IRI) model and available ionosonde data. Expected noise values at each site were generated using the International Telecommunication Union Radiocommunication Sector (ITU-R) radio noise model.

The goals of this work were to explore the consistency between the modeled and measured power of sky wave signals and noise levels. The initial results demonstrate that careful modeling supports a reasonable match to be achieved for this study case. At 3.33 MHz, an overall good match was achieved with some bias, which is thought to be a combination of receive gain modeling error and an overestimate of D region absorption. An overall excellent match was observed at 7.85 MHz, with a statistical spread in the measurements which reflects multipath channel characteristics not captured by the deterministic raytrace model. At 14.67 MHz, it was found that a modest match was achieved during the day, and a relatively poor match was observed at night due to the existence of interference not captured but the ITU-R noise model.

References

1. D. B. Francis, M. A. Cervera and G. J. Frazer, "Performance prediction for design of a network of skywave over-the-horizon radars," in *IEEE Aerospace and Electronic Systems Magazine*, vol. 32, no. 12, pp. 18-28, December 2017, doi: 10.1109/MAES.2017.170056.
2. Cervera, M. A., Francis, D. B., & Frazer, G. J. (2018). Climatological model of over-the-horizon radar. *Radio Science*, 53, 988– 1001. <https://doi.org/10.1029/2018RS006607>
3. Nickisch, L. J., St. John, G., Fridman, S. V., Hausman, M. A., and Coleman, C. J. (2012), HiCIRF: A high-fidelity HF channel simulation, *Radio Sci.*, 47, RS0L11, doi: 10.1029/2011RS004928.
4. Perry, G. W., Ruzic, K. D., Sterne, K., Howarth, A. D., & Yau, A. W. (2022). Modeling and validating a SuperDARN radar's Poynting flux profile. *Radio Science*, 57, e2021RS007323. <https://doi.org/10.1029/2021RS007323>
5. Conroy, J.P., Ellison, S., Wiker, J. R., Outwater, J., McFadden, F. (2023). Over-the-horizon (OTH) Ray Trace Model Anchoring. Paper presented at the National Radio Science Meeting in Boulder, CO.

Solar Cycle 25: Analysis of Recent Space Weather Events

Coster, Anthea J MIT Haystack Observatory

Aponte, Nestor, (MIT Haystack Observatory)

Zhang, Shun-Rong (MIT Haystack Observatory)

Goncharenko, Larisa, (MIT Haystack Observatory)

Derghazarian, Sevag, (MIT Haystack Observatory)

Solar cycle 25 began in December 2019 and was predicted to have a sunspot range between 95 to 130 with the solar maximum occurring between 2023 and 2026. Although these predictions led people to forecast similar activity levels to solar cycle 24, observations from 2020 to 2023 have significantly exceeded the anticipated values. For example, during the first month of 2023, sunspot numbers were around 185, much higher than the peak values of 95 to 130 predicted. Also in January 2023, the daily F10.7 values exceeded 220 and there were 3 X class solar flares. One day in February 2023, the daily F10.7 exceeded 300. With this in mind, we will report on observed space weather activity in 2022 and 2023 related to these heightened activity levels. We will utilize data in the Madrigal database including the total electron content (TEC) observations from the global ground-based network of GNSS receivers and scintillation statistics obtained from networks of specialized GNSS receivers. These networks include: the NSF MRI Collaborative: Development of Monitors for Alaskan and Canadian Auroral Weather in Space (MACAWS), the Canadian High Arctic Scintillation Network (CHAIN), the Low-Latitude Ionospheric Sensor Network (LISN), and in the Istituto Nazionale di Geofisica e Vulcanologia (INGV) network. New software will be used to merge the GNSS TEC maps and scintillation observations. In addition, optical observations from the THEMIS all-sky imaging network which measure the auroral activity and Super-DARN convection maps will be incorporated into our analysis of recent space weather events. Recent solar flares, large 2022 and 2023 geomagnetic storms and sub-storms, and specific scintillation events associated with storm enhanced density plumes, tongues of ionization, and auroral substorms will all be analyzed. Observed differences in space weather activity between the hemispheres will be highlighted. We will also examine the role of the higher levels of solar activity (F10.7) in the development of space weather phenomena.

Storm Effects, High Latitude Structure & Irregularities

Interpreting the Doppler shift of Transionospheric HF radio waves

Danskin, Donald University of Saskatchewan

Gillies, Rob (University of Calgary)

Eyiguler, E. Ceren (University of Saskatchewan)

Pandey, Kuldeep (University of Saskatchewan)

Hussey, Glenn (University of Saskatchewan)

Yau, Andrew (University of Calgary)

The radio receiver instrument (RRI) on the e-POP/Swarm-E satellite is affected by the motion of the satellite causing a Doppler shift in the received frequency. Traditionally, to determine the Doppler shift, only the motion of the receiver relative to the transmitter is necessary. However, when traveling through a dispersive medium such as the ionosphere, especially for radio waves in the HF band, the changing refractive index needs to be considered. Using a raytracing method, the refractive index is determined for an electron density profile along the path of the radio waves from the ground transmitter to the satellite receiver. The refractive index less than 1.0 causes the phase fronts to slow down. The resultant Doppler shift is lower than expected for the free space case. RRI data is used to validate the raytracing model for the Doppler Effect.

HF Propagation & Systems

The Onset and Development of Nitric Oxide Production During ICME-Driven Storms

Delano, Kevin University of Maryland, Baltimore County (UMBC)

Oliveira, Denny (UMBC/Goddard Space Flight Center)

Zesta, Eftyhia (Goddard Space Flight Center)

Enhanced thermospheric nitric oxide (NO) production regulates the interplay of neutral mass density heating and cooling, which in turn affects neutral density predictions, a crucial component of satellite orbital drag forecasting. However, the onset of NO production and its subsequent spatiotemporal development during storm times remains poorly understood. Using the Sounding of the Atmosphere using Broadband Emission Radiometry (SABER) instrument on the Thermosphere, Ionosphere, Mesosphere Energetic Dynamics (TIMED) spacecraft, we investigate NO production during 13 moderate geomagnetic storms (minimum SYM-H between -50 and -100) and 8 severe storms (minimum SYM-H between -150 and -250). We find that for stronger storms (i.e., lower minimum SYM-H), NO production tends to peak and return to pre-storm levels more quickly than for weaker storms. We also present in-depth analysis of a particular severe storm in December 2006 and show that both the shock impact and arrival of the storm result in NO enhancements at high latitudes.

Storm Effects

Connections Between Stratospheric and Mesospheric Gravity Waves, Winds and Traveling Ionospheric Disturbances

Derghazarian, Sevag MIT Haystack Observatory

Goncharenko, Larisa P. (MIT Haystack Observatory)

Zhang, Shun-Rong (MIT Haystack Observatory)

Coster, Anthea J. (MIT Haystack Observatory)

Harvey, V. Lynn (University of Colorado Boulder, LASP)

Randall, Cora (University of Colorado Boulder, LASP)

We present evidence that stratospheric gravity waves (GWs) are imprinted on the thermosphere and ionosphere as an enhancement in TIDs by examining their correlation in time over several winters. The role of the stratospheric polar vortex, zonal and meridional wind components, and shears in the propagation of these GWs are investigated by evaluating their temporal correlations with TIDs.

Traveling ionospheric disturbances (TIDs) are ubiquitous in many types of ionospheric data during both disturbed and geomagnetically quiet time and are highly variable in space and time. They are a source of uncertainty in high frequency radio systems and Global Navigation Satellite Systems (GNSS). Since they can degrade space-based communication, navigation, and precise positioning, understanding them and being able to predict their occurrence is important not only from a scientific but also from a technological perspective.

We use data from the Atmospheric Infrared Sounder (AIRS) to locate stratospheric GW hotspots over Europe (at an altitude of ~ 35 km) during the winters of 2016/17, 2018/19, 2019/20, and 2020/21. We show that these hotspots are imprinted on the ionosphere in a wide range of latitudes (25-80oN) and longitudes (Europe, Asia, eastern and central US). We also examine the connection between higher altitude gravity waves (~ 50 -55 km) and TIDs by using CIPS (Cloud Imaging and Particle Size) data.

The state of the polar vortex is shown to play a major role in the propagation of GWs. A strong polar vortex occurs during the month of December 2016 followed by a weak vortex for the remaining winter months due to Sudden Stratospheric Warming (SSW), whereas a strong vortex dominates throughout the entire winter of 2019-2020. The occurrence of different combinations of GW activity and polar vortex intensity allows us to evaluate the impact of the vortex independently. Longitudinal and correlation plots are presented that illustrate the enhancement of TID amplitudes, and the increase in GW activity.

In addition to the stratospheric polar vortex, the stratospheric and mesospheric wind system is shown to modulate the upward propagation of GWs. This is suggested by strong temporal correlations between TID amplitudes at various midlatitude locations with zonal and meridional wind velocities obtained from the Modern Era Retrospective Analysis for Research and Applications, version 2 (MERRA2) system.

Space Weather Applications & Services

The importance of electric field in ions convergence and formation of sporadic E (Es) at the equatorial region

Didebulidze, Goderdzi Ilia State University, Center of Space Research, G. Tsereteli str. 3a, 0162 Tbilisi, Georgia G. Tsereteli

Dalakishvili, Giorgi (Ilia State University, Center of Space Research, G. Tsereteli str 3a, 0162 Tbilisi, Georgia);

Maya Todua (Ilia State University, Center of Space Research, G. Tsereteli str 3a, 0162 Tbilisi, Georgia);

Toriashvili, Lekso (Ilia State University, Center of Space Research, G. Tsereteli str 3a, 0162 Tbilisi, Georgia)

The importance of electric field in formation of sporadic E (Es) at the equatorial region is investigated both analytically and numerically. In the suggested theory, the electric field in the lower thermosphere of the equatorial region is competitive to the effects of neutral wind direction, value and shear on ions vertical convergence into Es-type high density thin layer. We show analytically that minimal negative values of vertical changes of the ions vertical drift velocity, which are necessary for ions convergence into a Es-type layer, is possible due to electric field.

We also noted the importance of the electric field value and direction (including its components) in formation of the sporadic E. The electric field, even it is homogeneous in the region of ions convergence, can cause ions convergence into a Es-type thin layer. The possibility of formation of the Es layer is demonstrated numerically in cases of presence of electric field with the vertical and zonal components.

We used the HWM14 data which also showed the importance of competitive effects of the electric field and neutral wind velocity in formation of the Es layers. Here it is also shown the decrease of the electric field effect and increase of the neutral wind (including zonal and meridional winds) factor from equatorial to mid-latitude regions.

The electric field also has an influence on the competitive roles of itself and the neutral wind in ions divergence. In the suggested theoretical model, the arbitrary wind velocity profile (including the vertical component), caused by atmospheric waves, can be taken into account. The possibility of theoretical prediction of the ions convergence/divergence processes at the regions, where they develop, shows that it is important to investigate the global distribution of molecular and heavy metallic ions in the lower thermosphere.

This study is supported by the Shota Rustaveli National Science Foundation of Georgia, Grant no. FR-21-22825.

Equatorial Irregularities

Ionospheric response to the 23–31 August 2018 geomagnetic storm in the Europe-African longitude sector using multi-instrument observations

Dugassa, Teshome *Space Science and Geospatial Institute, Ethiopia*

Nigussie Mezgebe (Space Science and Geospatial Institute Ethiopia)

John Bosco Habarulema (South African National Space Agency)

This study presents ionospheric responses of the mid and low-latitude region in the Europe-African longitude sector (along 30°E±10°E) to the intense geomagnetic storm of 23-31 August 2018 (SYM-H_{min} = -207 nT) using the Global Ionospheric Map (GIM) and Global Positioning System (GPS) receivers data, the satellite data (SWARM, Defense Meteorological Satellite Program (DMSP), Global Ultraviolet Imager on board the Thermosphere, Ionosphere, Mesosphere Energetics and Dynamics (GUVI/TIMED)), and Prompt Penetration Equatorial Electric Field model (PPEFM). The percentage deviation in total electron content (TEC) denoted by DTEC (%) was used to observe the ionospheric storm effects. The rate of change of TEC index (ROTI) derived from GPS-TEC and the rate of change of plasma density index (RODI) obtained from SWARM satellites were utilized to quantify the occurrence of ionospheric irregularities. Results obtained from GPS receivers and GIM data revealed a large increase in TEC (positive ionospheric storm effect) in the equatorial and low-latitude region of Africa, and a decrease in TEC (negative ionospheric storm effect) over the midlatitude region of Europe and Africa during the storm recovery phase. The decrease in $\frac{1}{2}O=\frac{1}{2}N^2$ ratio is the possible cause for the observed negative ionospheric storm effect. Hemispheric asymmetry were noticed over Europe-African longitude sector during the storm main and recovery phases. The occurrence of ionospheric irregularities over the low-latitude region of Africa in the pre-midnight and post-midnight was suppressed (ROTI < 0.4 TECU/min). This could be related to the local time at which the minimum SYM-H occurred which corresponded to daytime over Europe-African longitude sector. This, on the other hand, may not support the development of conducive environment for the generation of ionospheric irregularities. However, significant fluctuation in the plasma density was noticed by the SWARM-C on 23, 25, 30, and 31 August 2018 over equatorial and low-latitude region of Africa during the post-midnight period

Storm Effects

Combining Ground- and LEO-RO-Based GNSS Observations in Real-time Operational Space Weather Products

Durgonics, Tibor^{1,2}, Tzu-Wei Fang¹, Terry Onsager¹, Frank Centinello¹, Jun Wang², Dominic Fuller-Rowell^{1,2}, Mihail Codrescu¹

¹NOAA Space Weather Prediction Center

²Cooperative Institute for Research in Environmental Sciences, CU Boulder

NOAA's Space Weather Prediction Center (SWPC) has responsibility for continuously monitoring, forecasting, and alerting on conditions in the Earth's space environment that impact our technological infrastructure and human health and safety. One of the main space weather products is the ionosphere specification. Ionospheric density changes impact our technologies utilizing global navigation satellite systems (GNSS) and signals propagating between satellites and the ground stations as it can cause signal delays and disruptions. SWPC focuses on improving existing and creating new real-time, operational products of the two main ionospheric descriptive quantities: total electron content (TEC) and ionospheric scintillations. SWPC is also one of the centers that are responsible for space weather services identified by the International Civil Aviation Organization (ICAO). The ionospheric models developed at SWPC target GNSS and HF communication advisories. A new real-time specification tool being developed will support the decision making at the forecast office on more accurate GNSS advisories in the near future.

The current ionospheric TEC and scintillation products, such as 2D TEC maps and rate of TEC index (ROTI) maps, have been derived from ground-based GNSS measurements. The exclusively ground based approach has its advantages and disadvantages. One of the prominent disadvantages is that it cannot provide observations over, e.g., oceans and remote areas. Empirical ionospheric models and various smoothing and interpolating techniques have been used to fill these coverage gaps. The introduction of GNSS receivers to low-earth-orbit (LEO) satellites represented a breakthrough, since they allowed GNSS observations to be performed anywhere globally regardless of ground conditions, permitting to perform radio occultation (RO) type remote sensing of the ionosphere, in a so-called limb-sounding geometry (GNSS-to-LEO satellites). The computed excess phase can be used for deriving TEC, ROTI, and phase scintillation (σ_ϕ) calculations, while the rapid changes in the signal's carrier-to-receiver noise density ratio or signal-to-noise characteristics allow for the calculation of the amplitude scintillation index (S_4). Ground-based (disc-sounding geometry) GNSS measurements can also be used to infer the ionospheric TEC and scintillation indices. Therefore, the combination of these limb- and disc-geometry observations should, in theory, provide a more complete global coverage than any of the single geometries alone. The existing ground GNSS networks in combination with the increasing number of RO-capable LEO satellites and constellations may provide better ionospheric products and finer resolutions both spatially and temporally. RO data covering low- and mid-latitudes are available from the COSMIC-2 constellation, while commercial data providers are able to deliver global data from polar orbiting satellites. However, the combination of these two measurement geometries is not trivial, and some fundamental physical questions need to be answered before it can be implemented into a practical application.

SWPC's plan is to combine ground- and space-based measurements to build improved real-time operational products of ionospheric TEC and scintillations. These products will be used to monitor the ionosphere and provide alerts for potential disruptions to radio communication and

navigation, thus providing society with actionable space weather information. The main challenges are currently being addressed in close collaboration with Boston College and Aerospace Corp.: 1) the validation of ground-based scintillation measurements, 2) geolocation of RO scintillation events and 3) the determination of the limb-to-disc conversion algorithm between ground- and RO-based scintillation magnitudes. There are established methods to geolocate scintillation events along a given signal-path for ground observations, but the magnitude can depend significantly on the direction of the signal propagation in relation to the plasma structures. On the other hand, the RO geolocation algorithm that could cover all latitudes is still being researched and developed. Furthermore, performing a physically sound limb-to-disc conversion of the measurement magnitudes is necessary due to the different geometries of the measurements, which cannot be interpreted together without such a conversion. This has not been completed yet and requires additional work, especially for high-latitudes.

Further challenges arise from the fact that the ionosphere is a non-linear, dynamic, and complex system, which makes its modeling, forecasting and even nowcasting quite an intricate task. Both the RO and ground-based GNSS measurements are subject to errors which need to be taken into account and continuously estimated. Such a complex, real-time system and operational product must be updated frequently because data and processing latencies can significantly affect the quality of the service and the ability to base decisions on its output.

Despite the challenges, the benefits of using a real-time operational ionospheric product outweigh the costs. This product can be used to improve the safety and reliability of radio communications and navigation globally. It can lead to improved situational awareness of the ionosphere, early warning capability and improved decision-making for mitigation of ionospheric disruptions.

Topside Ionosphere Electron Density Modeling with Empirical and Machine Learning Techniques

Dutta, Shweta Georgia Institute of Technology

Cohen, Morris (Georgia Institute of Technology)

This research focuses on modeling the electron density in the topside of the ionosphere with a combination of a developed machine learning model and existing empirical models, specifically the International Reference Ionosphere (IRI) and the Empirical-Canadian High Arctic Ionospheric Model (E-CHAIM). In prior work, an artificial neural network (NN) was developed and trained on two solar cycles worth of Defense Meteorological Satellite Program (DMSP) data (113 satellite-years), along with global drivers and indices to predict topside electron density. We tested the model on six years of subsequent data (26 satellite-years) and found a correlation coefficient of 0.87 between the model predictions and the DMSP electron density data. While the NN model outperforms the IRI when tested on data in the altitude range the NN was trained on, performance is degraded in the polar region and during elevated solar activity when testing on a dataset sourced from a lower altitude satellite. Now, we present analysis of the matured NN model, E-CHAIM, and IRI by geographic location and geomagnetic condition within the topside ionosphere, and preliminary work to combine all three models via stacked generalization.

Topside & Plasmasphere

Global Observations of Sporadic-E and Spread-F Occurrence Rates Using the COSMIC-2 Constellation

Dymond, Kenneth Naval Research Laboratory

We observed the presence of ionospheric L-band Sporadic-E and Spread-F occurrence during 2020-2022 using the Constellation Observing System for Meteorology, Ionosphere, and Climate – 2 (COSMIC-2) also known as FORMOSAT-7. We used the reported S4 scintillation index, an indicator of the scintillation along the line-of-sight, and following previous studies, geolocated the scintillation to the tangent ray height of the line-of-sight between the COSMIC-2 satellite and the Global Positioning System satellite. We then produced maps of the scintillation occurrence frequency versus season and time of day. Our results are in agreement with prior studies using the COSMIC-1 satellites, but some features are more clearly seen in our study. We compare our results with observations of ionospheric bubbles made by the Global-Scale Observations of the Limb and Disk (GOLD mission [Eastes, et al. (2017), “The Global-Scale Observations of the Limb and Disk (GOLD) Mission”, Space Sci. Rev., doi: 10.1007/s11214-017-0392-2.] and to other ionospheric observations.

Scintillation & Propagation Effects on GNSS and Other Systems

The Experiment for Characterizing the Lower Ionosphere and Prediction Sporadic-E (ECLIPSE) Missions: Instruments to Study the Dynamics of the Lower Ionosphere

Dymond, Kenneth F. U.S. Naval Research Laboratory

Andrew C. Nicholas, Bruce A. Fritz, Scott A. Budzien, Andrew W. Stephan, Charles M. Brown, Ellen J. Wagner, Meghan R. Burleigh, and Douglas P. Drob

U.S. Naval Research Laboratory, 4555 Overlook Ave, Washington, DC, 20375, USA.

The Naval Research Laboratory designed and developed small instruments for flight on CubeSats to study the Earth's ionosphere. One instrument is a photometer, called the Triple-Tiny Ionospheric Photometer (Tri-TIP), used to measure the brightness of the O I 135.6 nm emission produced primarily by radiative recombination of O⁺ ions and electrons. At nighttime this emission can be used to infer the distribution of electrons in the ionosphere. A second instrument, called the Triple-Magnesium Ion Photometer (Tri-MIP), is designed to measure the Mg II 280 nm emission, which is produced during the daytime by scattering of sunlight by Mg⁺ ions in the ionosphere. Mg⁺ ions are produced by meteoric ablation and also by charge exchange between molecular ions and Mg atoms produced during the meteor ablation. Mg⁺ ions act as tracers of the dynamical drivers in the E-and F-regions of the ionosphere. Prior measurements of both species have been used to determine the two-dimensional distribution of the ions in the orbit plane of the satellite making the measurements.

In this talk, we will describe the observations of the Tri-TIP and Tri-MIP instruments on two missions. A prototype of the Tri-MIP instrument was built and launched on a new CubeSat mission (ECLIPSE-RR) into low Earth orbit to study the spatial distribution of Mg⁺ ions. The satellite (SLINGSHOT-1), a collaboration with the Aerospace Corporation, was launched out of Southern California on the Virgin Orbit launch that occurred on July 2, 2022. The orbit is near circular at an altitude of 555 km and an inclination angle of 45°. The second mission, ECLIPSE, will fly two Tri-MIPs and two Tri-TIPs on the United Space Force Space Test Program's STP-H9 mission that is slated to be launched to the International Space Station on March 11, 2023. The ECLIPSE mission features one Tri-TIP and one Tri-MIP with scanning mirrors that will scan the Earth's limb behind the ISS to make limb scans versus altitude in the orbit plane of the ISS. The mission also includes one Tri-TIP and one Tri-MIP viewing downward beneath the ISS and scanning cross-track to make 2D observations over the globe. In this presentation, we discuss the missions, describe the ECLIPSE instruments, and present early mission results showing both the horizontal structures and the distribution of Mg⁺ and O⁺ ions in the satellite's orbit plane and make comparisons to a coupled ionosphere/thermosphere model." Optical

Remote Sensing

Comparisons of the Data-Driven D Region (D3R) Model to Incoherent Scatter Radar Observations During the Active Solar Conditions of September 2017

Egert, Austin *Space Dynamics Laboratory*

Eccles, James V., *Space Dynamics Laboratory*;

Holmes, Jeffrey M., *Air Force Research Laboratory*;

Malins, Joseph, *Air Force Research Laboratory*

The physics-based Data-Driven D-Region (D3R) model calculates electron density profiles from 40 to 130 km for quiet time and disturbed conditions. The D3R model has recently been updated with the following: (1) additional positive and negative ions, similar to the 8-component scheme of Bekker et al. (2022), (2) updated reaction rates presented in Pavlov (2014, 2015), (3) the Flare Irradiance Spectral Model-Version 2 (Chamberlin et al., 2020), and (4) the NRLMSIS 2.1 neutral atmosphere (Emmert et al., 2022). The D3R model calculates the electron-neutral collision frequency, which we use to calculate the High-Frequency (HF) absorption using the procedures presented in Zawdie et al. (2017).

We compare D3R E and D region electron density profiles and HF absorption predictions against observations of available Incoherent Scatter Radar (ISR) observations during the active solar period of September 2017. Data from the Millstone Hill ISR, Arecibo Observatory ISR, and Poker Flats ISR provide electron density profiles during September 2017.

Bekker, S. Z., S. I. Kozlov, and V. P. Kudryavcev (2022). Comparison and verification of different schemes for the ionization-recombination cycle of the ionospheric D-region, *Journal of Geophysical Research Space Physics*, 127, e2022JA030579.
<https://doi.org/10.1029/2022JA030579>

Chamberlin, P. C., F. G. Eparvier, V. Knoer, et al. (2020). The Flare Irradiance Spectral Model-Version 2 (FISM2), *Space Weather*, 18(12), e2020SW002588.
<https://doi.org/10.1029/2020SW002588>

Emmert, J. T., Jones, M. Jr., Siskind, D. E., Drob, D. P., Picone, J. M., Stevens, M. H., et al. (2022). NRLMSIS 2.1: An empirical model of nitric oxide incorporated into MSIS. *Journal of Geophysical Research: Space Physics*, 127, e2022JA030896.
<https://doi.org/10.1029/2022JA030896>

Pavlov, A. V. (2014). Photochemistry of Ions at D-region Altitudes of the Ionosphere: A Review, *Surveys in Geophysics*, 35, 259-334.
<https://doi.org/10.1007/s10712-013-9253-z>

Pavlov, A. V. (2015). Erratum to: Photochemistry of Ions at D-region Altitudes of the Ionosphere: A Review, *Surveys in Geophysics*, 36, 623-625. <https://doi.org/10.1007/s10712-015-9328-0>

Zawdie, K. A., D. P. Drob, D. E. Siskind, and C. Coker (2017), Calculating the absorption of HF radio waves in the ionosphere, *Radio Science*, 52, 767-783,
<http://doi.org/10.1002/2017RS006256>

Approved for public release; distribution is unlimited. Public Affairs release AFRL-2023-0740.

The views expressed are those of the authors and do not reflect the official guidance or position of the United States Government, the Department of Defense or of the United States Air Force.

Statement from DoD: The appearance of external hyperlinks does not constitute endorsement by the United States Department of Defense (DoD) of the linked websites, or the information, products, or services contained therein. The DoD does not exercise any editorial, security, or other control over the information you may find at these locations."

HF Propagation & Systems

Operational Assimilative Ionospheric Models in Europe and the UK

Elvidge, Sean SERENE, University of Birmingham

Themens, David (SERENE, University of Birmingham)

Comprehensive, global and timely specifications of the Earth's ionosphere is required to ensure the effective operation, planning and management of a diverse range of systems impacted by space weather. This year, a number of national space weather operational centres are deploying ionospheric data assimilation models operationally.

The UK Met Office Space Weather Operations Centre (MOSWOC) run the Advanced Ensemble electron density (Ne) Assimilation System (AENeAS), a physics-based data assimilation model of the coupled ionosphere-thermosphere system. AENeAS assimilates data using the local ensemble transform Kalman filter (LETKF) into a background model (the Thermosphere Ionosphere Electrodynamics General Circulation Model [TIE-GCM]). The model provides probabilistic environmental nowcasts and forecasts, as well as tailored products and services to support industry and Government.

The European Space Agency's Space Weather Service Network will run the Advanced Ionospheric Data Assimilation (AIDA) model pre-operationally. AIDA uses a modified Auxiliary Particle Filter to assimilate data into the climatological NeQuick model. Unlike most global data assimilation models, AIDA uses basis functions as its state space to drastically reduce its size and describes the forward model via analytical functions rather than discrete voxels. These computational savings allow for the use of a more intensive assimilation method, for example APFs, which are more flexible and can incorporate highly non-linear datasets.

Space Weather Applications & Services, Assimilative and Coupled Models

Ionospheric Profile Retrievals using 1D-Var with COSMIC-2 Bending Angles

Elvidge, Sean SERENE, University of Birmingham

Culverwell, Ian D (Met Office, UK)

Healy, Sean B (European Center for Medium-Range Weather Forecasts)

This paper describes, and validates, a technique of retrieving ionospheric profiles using a 1D Variational (1D-Var) assimilation system using bending angles derived from FORMOSAT-7/COSMIC-2 data. Traditionally when assimilating slant total electron content (STEC) observations into ionospheric data assimilation models an estimate of the Differential Code Biases (DCBs) are required. These can be estimated by the data provider or, alternatively, DCBs are commonly estimated during the assimilation step in many models by including them in the state vector. However the uncertainty in the DCB estimation, and its impact on the final analysis, is often overlooked.

To overcome the challenge of DCB estimation in this work the L2 minus L1 bending angles have been assimilated. Using a simple “Vary-Chap” model with a 1D-Var retrieval code, assimilating the bending angles, ionospheric profiles are reconstructed. These retrievals are compared to the Level 2 F7/C2 products and validated against ionosonde observations. The study looks at all COSMIC-2 retrievals within 200 km of an ionosonde with “well”-scaled ionograms from 2020. The 1D-Var retrieved bottomside profiles results in an improvement, compared to ionosonde observations, over the COSMIC-2 electron density profiles by approximately 40%.

Radio Occultations & Tomography

Attitude effects on the observed orientation angle of HF waves from the Radio Receiver Instrument on e-POP/Swarm-E

Eyiguler, E. Ceren University of Saskatchewan

Danskin, Donald W. (University of Saskatchewan)

Howarth, Andrew D. (University of Calgary)

Holley, Warren (University of Calgary)

Pandey, Kuldeep (University of Saskatchewan)

Gillies, Robert G. (University of Calgary)

Yau, Andrew W. (University of Calgary)

Hussey, Glenn C. (University of Saskatchewan)

The Radio Receiver Instrument (RRI) on e-POP/Swarm-E has a cross-dipole antenna capable of observing HF radio waves. Slew-to-transmitter passes, in which the antenna boresight direction is aligned with the ray direction are the ideal cases to observe the full polarization ellipse. From the voltages on the dipoles, the polarization characteristics, such as the ellipticity angle and the orientation angle can be determined. However, the RRI may not always be in an optimum position to observe the full signal. In such cases, the polarization characteristics cannot be fully captured. In this work, the effects of dipole boresight pointing on the observed orientation angle during Faraday rotation periods and the preliminary studies to recover the original signal polarization characteristics will be presented.

HF Propagation & Systems

Assimilative Modeling of the Ionospheric Layers

Forsythe Victoriya *NRL*

McDonald, Sarah (NRL), Kuhl, David (NRL), Fritz, Bruce (NRL), Diamond, Ken (NRL)

A new data assimilation (DA) scheme for the parametrized ionospheric electron density is currently under development at the Naval Research Laboratory (NRL). It provides the nowcast for the given ionospheric background model influenced by ionospheric observations, using sequential Kalman Filter on the maps of the ionospheric parameters in Quasi-Dipole-MLT coordinate system. During this presentation, this new DA scheme, the covariance formation and the data aggregation will be introduced. The pre-processing technique for three data types, ionosonde, radio occultation, and ground-based GPS data, will be described. First results and preliminary validation efforts, including the comparison with IDA4D results will be demonstrated.

Distribution Statement A. Approved for public release. Distribution is unlimited.

This work is sponsored by the Office of Naval Research.

Assimilative and Coupled Models

First-year Results from a Space-based Sporadic-E Detector

Fritz, Bruce U.S. Naval Research Laboratory

Dymond, Kenneth (U.S. Naval Research Laboratory),

Nicholas, Andrew (U.S. Naval Research Laboratory),

Budzien, Scott (U.S. Naval Research Laboratory),

Stephan, Andrew (U.S. Naval Research Laboratory)

The Triple Magnesium Ionospheric Photometer (Tri-MIP) has been developed as a 1U CubeSat compatible sensor to detect a mid-ultraviolet (MUV), Mg⁺ doublet emission near 280 nm as a tracer of Es. The initial flight of Tri-MIP is on the Slingshot-1 spacecraft that launched into a circular orbit at an altitude of 500 km and an inclination of 45°. Paired with a 1U scanning ultraviolet mirror (SUV) on the Slingshot-1 spacecraft, Tri-MIP provides altitude profiles of Mg⁺ airglow emissions through limb scans of Earth's ionosphere along the wake direction of the orbit. Tri-MIP is especially well-suited for Es detection and may allow for the observation of faint signatures of Es that are otherwise not visible with other commonly used, remote plasma detection methods, such as ground-based ionosondes or GPS radio occultation experiments. This will show the data reduction approach that is being applied to the observations as well as a summary of results from the first year of operations on orbit.

Natural & Artificial Anomalous Events, Optical Remote Sensing, Radio Occultations & Tomography

The Incorporation of Near Real Time Ionospheric Propagation Information for Automated Link Establishment Based Communication Systems

Furman, William L3Harris Technologies, Inc.

Batts, William (L3Harris Technologies, Inc.)

Buckley, Richard (L3Harris Technologies, Inc.)

Nieto, John (L3Harris Technologies, Inc.)

This paper focuses on the use of the HF frequency band, 3-30 MHz, as a wireless communications medium where the predominant propagation mode is provided by ionospheric refraction. The HF medium provides a reliable mode of long distance, beyond line of sight, communications used by many nations and entities worldwide.

The paper begins with an overview of existing Automated Link Establishment (ALE) systems which provide a mechanism to find the best propagating frequency between any radios on earth and to set up the radios for communication. The paper will provide a brief history of ALE throughout the years up to and including the current U.S. MIL-STD-188-141D.

Next the use of propagation prediction software is discussed with a concentration on VOACAP. This package provides a prediction of the best propagating frequency between points on earth based many factors including geographic positions, time of day, solar activity, and noise conditions. VOACAP is generally used to select possible / probable frequencies to use before radios are deployed in the field but does not have a mechanism to address real time variations in propagation.

Sources of Near Real Time (NRT) propagation information are then discussed . This information includes WWV broadcasted geomagnetic and solar indices information, inputs from space weather organizations, and amateur radio propagation probing waveforms such as WSPR.

A comparison of various waveforms for real time channel evaluation is then presented. Examining waveforms used by the US MIL-STD ALE, WSPR and previous experiments.

A Machine Learning (ML) based consolidation model combining the above information is then presented including comparison of the model to both VOACAP predictions and real world measured propagation measurements.

Finally an enhanced ALE based system is presented based on the current MIL-STD (4G ALE) combined with all the previously discussed Near Real Time information and Machine learning based models. The best way to validate this approach experimentally is discussed and the potential way forward is outlined.

HF Propagation & Systems

A Vertically-Resolved Model for Ionospheric Absorption of HF radio waves due to solar protons and X-rays

Goertz, Anton Los Alamos National Laboratory

Jeffery, Christopher (Los Alamos National Laboratory)

High Frequency (HF) skywave radio signals are used in various communication technologies and commonly pass through the D-Region ionosphere. Enhanced levels of D-Region ionization during geomagnetic storms can cause partial or even complete absorption of HF radio waves leading to communication disruptions and blackout. This ionization is predominantly caused by solar energetic protons (SEP) and solar X-rays precipitating into the ionosphere. To better predict this process, we have developed a new vertically-resolved model to determine the absorption of HF waves due to SEPs and solar X-rays. Our model explicitly resolves the altitude-dependence of high-energy particle deposition, D-Region ionization, and enhanced RF signal attenuation. The model input is the energetic proton and X-ray flux spectrum as measured by the EPEAD instrument and X-ray sensor on the GOES satellite constellation. We compare modeled absorption time-series to absorption measurements made by riometers in the Canadian High Arctic Ionospheric Network (CHAIN). Furthermore, we also compare the performance of our model against the widely used NOAA D-region absorption prediction (D-RAP) algorithm. The D-RAP algorithm was empirically derived by establishing a quantitative relationship between riometer absorption and solar proton and solar X-ray flux measurements. It uses the same data input as our model.

Storm Effects, HF Propagation & Systems, Radio Occultations & Tomography

Reconstruction of the Electron Precipitation Spectrum Based on Modeling of Auroral Optical Emission Tomography

Goertz, Anton Los Alamos National Laboratory

Whiter, Daniel (University of Southampton)

Electron precipitation spectra are quite variable spatially and temporally, which is why accurate and localized measurements of electron precipitation spectra are required and typically only available by direct Low-Earth-Orbit (LEO) satellite measurements. The Defense Meteorology Satellite Program (DMSP) satellite constellation offers measurements of electron precipitation spectra at relatively high energy resolution between 30 eV and 30 keV. The inherent disadvantages associated with electron flux data from any LEO satellite are that they have very limited data coverage for any single location, and that the high speed of satellites introduces a tradeoff between spatial resolution and the minimization of statistical errors of the electron flux data. These disadvantages are bypassed when using auroral inversion techniques. We present a model based on first principles that can determine auroral tomography using an electron flux spectrum as its input. We validated our model by reproducing altitude emission profiles extracted from ASC images. We use multiple spectra measured by DMSP satellites to calibrate an inversion algorithm which uses auroral emission profiles as its input to determine electron flux spectra. While simulation of most auroral emissions requires the precise modeling of thermospheric chemistry, obtaining the auroral tomography of the blue nitrogen line is simpler as there is only a single dominant production reaction. Hence, our model is based on the nitrogen emission line. Our inversion algorithm enables estimation of electron flux spectra at any location and time for which there is ASC data available, which circumvents many of the issues associated with local data coverage of space based measurements.

High Latitude Structure & Irregularities, Optical Remote Sensing

An Empirical Mid-Latitude Model of the CkL Irregularity Index from 35 MHz Scintillation Data

Helmboldt, Joseph U.S. Naval Research Laboratory

Hicks, Brian (U.S. Naval Research Laboratory)

Coombs, Joseph (U.S. Naval Research Laboratory)

Taylor, Gregory (University of New Mexico)

Dowell, Jayce (University of New Mexico)

This paper summarizes work focused on improving the ability to assess and predict the level of km-scale ionospheric irregularities at mid-latitudes based on a recently developed capability to measure 35 MHz scintillations using cosmic radio sources. The Deployable Low-band Ionosphere and Transient Experiment (DLITE) is a low-cost, interferometric radio telescope consisting of four inverted vee-shaped dipole antennas developed for the Long Wavelength Array (LWA) project. Unlike telescopes like the LWA, which are designed to maximize sensitivity for astrophysical investigations, DLITE is optimized for ionospheric remote sensing and affordability/ease of deployment to facilitate widespread geographical coverage. The telescope resolves multiple exceptionally bright cosmic radio sources (2-4 at a time) in a 30-40 MHz band using time and frequency difference of arrival methods rather than beam forming. This is made possible by separating the antennas by ~200-500 m and using a bandwidth of ~8-10 MHz. The apparent position and intensity of each source is monitored to characterize gradients in the line-of-sight total electron content and scintillations due to km-scale irregularities (Fresnel scale is ~1-2 km). The system and methods developed to convert these scintillation measurements to the frequency- and geometry-independent CkL irregularity index are described in detail by Helmboldt et al. (2021. *Radio Science*, 56, e2021RS007298).

In the autumn of 2019, DLITE arrays were established in southern Maryland near the town of Pomonkey (DLITE-POM) and in New Mexico at the site of the Very Large Array (DLITE-NM). A third array was installed at Malabar Annex Space Force Base in Florida near the end of 2021 (DLITE-FL). Examination of CkL measurements from DLITE-POM and DLITE-NM over many months revealed that they were well correlated with a delay of ~2 hours. This is the expected result if CkL depends more strongly on local solar time rather than location. Armed with this knowledge and a modest network of three DLITE arrays, an empirical model was developed for $\log_{10}\text{CkL}$ based on spherical harmonics as functions of latitude and local time. An additional term was added to allow the mean $\log_{10}\text{CkL}$ to vary linearly from day-to-day without changing the local time/latitude dependence, which facilitates forecasting. It was found that using the previous ~5-7 days of data produced reasonable nowcasts and three-day forecasts.

The details of the data and the methods used will be discussed along with tests of validity/utility. The latter consists of an examination of detections of backscatter from meter-scale irregularities with the Blackstone, Virginia SuperDARN radar (BKS) with predictions of CkL from the DLITE-based models and the climatological Wideband Model (WBMOD) for the period spanning 11 Dec. 2021 through 20 Jun. 2022. It will be demonstrated that there is a clear correlation between backscatter signal-to-noise ratio detected with BKS and CkL calculated with

the DLITE-based model at the irregularity locations. This trend is not present when WBMOD CkL values are used. While the two measurements probe different portions of the irregularity spectrum, this result still indicates that utilizing up-to-date regional scintillation data can improve irregularity nowcasting and forecasting at mid-latitudes.

Scintillation & Propagation Effects on GNSS and Other Systems

Simultaneous Measurements of Temporal and Spatial Phase Structure Functions of an HF Skywave Signal at Mid-Latitudes

Helmboldt, Joseph *U.S. Naval Research Laboratory*

This paper presents the results of a test data collection with an HF/VHF interferometer in southern Maryland of the skywave propagating signal from WWV near Ft. Collins, Colorado. For HF applications that utilize skywave propagation, km-scale irregularities within the ionosphere distort the ray paths resulting in phase and amplitude errors that can negatively impact performance. Thus, both the coherence time and coherence length of any skywave channel are important quantities as they define the best achievable Doppler and angular resolutions, respectively. Using a four-antenna interferometer with spacings of ~100-350 m near Pomonkey, Maryland, a four-hour test data collection was made of the 10 MHz signal from WWV in Feb. 2020. This paper presents an analysis of the temporal and spatial phase structure functions (SFs) from this collection to constrain the coherence time and length as well as the relationship between the two.

Exploiting the WWV carrier wave, temporal SFs were measured from each individual antenna. Arrival times of the WWV on-the-second pulse indicated two-hop propagation for the first 1.3 hours of the collection starting at 22 UT on 14 Feb. 2020. Following this, the arrival times indicated a one-hop path for the next ~2.5 hours after which the channel disintegrated near sunset. The SFs indicated that the coherence times for the two-hop signals were ~1-2 s. As expected, the coherence times for the one-hop signals were somewhat larger at ~2-4 s prior to sunset. Near sunset, the coherence times dropped to ~1 s or below. Beyond the inner portions of the SFs that were power-law shaped (i.e., separations larger than ~5 s), there were often quasi-periodic structures with nodes separated by a few seconds to ~20 s.

Spatial SFs were measured by examining cross correlations of the signals among the six unique pairs of antennas, or “baselines.” The baseline lengths spanned a region that was wide enough to measure the shape of inner portion of the SF and consequently the coherence length. However, nearly all of these spatial SFs were power-law shaped, indicating that the outer scale was typically larger than the longest baseline of ~350 m. Before sunset, the ratio of the coherence length to the coherence time was ~220 m s⁻¹ for both two- and one-hop signals. Within this timeframe, the ratio partially exhibited periodic behavior with a period of ~40-45 minutes and amplitude of ~35 m s⁻¹. Near sunset, the ratio increased to ~400-800 m s⁻¹ and was highly variable.

The implications of these measurements for modeling both Doppler and angular broadening of skywave signals will be discussed with some emphasis on over-the-horizon (OTH) radars. The impact during instances where the coherent integration times used are long enough to reach the regime where the SF is quasi-periodic is of particular interest.

HF Propagation & Systems

Data-Assimilative Ionospheric Profile Specification Using Scaled IRI Parameters

Hoskinson, A. R., V. Paznukhov, W. J. McNeil, M. Proctor, C. S. Carrano, and K. M. Groves
Institute for Scientific Research, Boston College

We present a regional data-assimilative ionospheric model, the Region Ionospheric Profile Estimator (RIPE) that aims to improve the specification of bottom-side electron density profiles by updating individual profile parameters of the International Reference Ionosphere (IRI) based on measured ionosonde data. Our approach operates on the *ratios* of auto-scaled parameters to climatological model predictions for f_oF2 (URSI model), $hmF2$ (Shubin), and B_0 and B_1 (Altadill, Torta, and Blanch). This approach allows the dominant spatial and temporal structure in the ionosphere to be handled by well-validated climatological models, while the data assimilation routines handle only the deviations from climatology. These deviations are much closer to normally-distributed than the profile parameters themselves. The use of specific profile parameters rather than effective solar indices enables a more detailed specification of bottom-side profiles, and is extensible to additional parameters as desired. We show spatial correlations for filtered measurement ratios over several geographic regions and time periods, which generally exhibit length scales on the order of 2000 km. Validation exercises demonstrate significant improvement over pure climatological model runs, and are relatively insensitive to precise choice of correlation lengths.

The views expressed are those of the authors and do not reflect the official guidance or position of the United States Government, the Department of Defense or of the United States Air Force.

Approved for public release; distribution is unlimited.

Assimilative and Coupled Models

Modeling Plasmasphere Structure: Ducts and Irregularities

Huba, Joe Syntek Technologies

Liu, H.-L., HAO

Becker, E., NWRA

We present results from high-resolution simulations of the thermosphere-ionosphere-plasmasphere system using the coupled SAMI3/WACCM-X and SAMI3/HIAMCM models. We show that atmospheric gravity waves can generate plasma irregularities and ducts in the plasmasphere. High resolution simulations using SAMI3 with the empirical models NRLMSISE00 and HWM14 of the thermosphere do not show any density structuring. We demonstrate that field-aligned ducts (i.e., localized density enhancements or reductions) can form in the mid-latitude ionosphere by calculating the flux-tube integrated total electron content (in contrast to vertical total electron content). We find that there can be variations of a few percent over a few degrees in longitude. We also discuss how these results may apply to plasmasphere irregularities observed by radio astronomy facilities as well as to VLF propagation studies.

Topside & Plasmasphere

A Verification and Validation of the Observation System Simulation Experiment Tool

Hughes, Joe Orion Space Solutions

Collett, Ian (Orion Space Solutions)

Reynolds, Adam (Orion Space Solutions)

Crowley, Geoff (Orion Space Solutions)

Decision makers are often tasked with choosing how many sensors to deploy, of what types, and in what locations to meet a given operational or scientific outcome. An Observing System Simulation Experiment (OSSE) is a numerical experiment which can provide critical decision support to these complex and expensive choices. There are three steps in an OSSE:

- (1) An observation system consisting of any combination of instruments such as ionosondes, GPS ground stations, satellite-based RO is specified and the measurements are simulated using the truth model which contains the electron density at every location and time.
- (2) These simulated measurements are provided to an assimilator which uses them to update a background model and create an analysis.
- (3) The analysis and the background model are compared to the truth model. The degree to which the analysis improves relative to the background indicates the value of those measurements. This process can be repeated for multiple combinations of instruments to compare the relative impact of different data sets. This impact can be paired with the cost of these datasets to estimate the ionospheric specification “bang” for a real-life buck.

Orion Space Solutions has developed the OSSE Tool (OSSET) which is a set of software used to perform ionospheric OSSEs. To our knowledge, it is the first such tool of its kind. This has two parts. First, we describe OSSET's basic operation and what data sets it can simulate. Second, we compare OSSET's predictions of the impact of adding Radio Occultation TEC data to the real impact of adding RO data.

Space Weather Applications & Services

MF Scattering from the Exponential D-Region: Analytic Theory & Double-Peaked Ground Signatures

Jeffery, Christopher Los Alamos National Laboratory

MF Scattering from the exponential D-Region is investigated analytically using the geometrical optics approximation. Expressions for scattered-ray path and amplitude are derived and used to interpret results of frequency-domain full-wave simulations with km-scale regions of imposed stochastic variability. The simulations reveal double-peaked ground signatures that appear consistent with the dual Doppler structures seen by Obenburger et al. (Radio Science, 2022). Analysis reveals that the far peak is due to refraction, while the near (transmitter-ward) peak is caused by scattering of rays that first ionospherically reflect. The contribution of horizontal, near-caustic scattering to the latter peak from plasma variability at the reflection height is further clarified.

HF Modeling, TIDs and Geolocation

Development of an Autonomous RF System that exploits SuperDARN Signals for Bistatic Radar Imaging of High-Resolution Ionospheric Structures near HAARP

Jeffery, Christopher Los Alamos National Laboratory

Shao, Xuan-Min (LANL)

Beveridge, Andrew (LANL)

Cummings, Ian (LANL)

Cunningham, Greg (LANL)

Fallen, Christopher (AFRL)

Haynes, Brian (LANL)

Lay, Erin (LANL)

Nelson, Eric (LANL)

Reisner, Jon (LANL)

Rushton, Jeremiah (LANL)

Los Alamos National Laboratory is developing a new bistatic coherent radar imaging system for deployment near HAARP, that leverages decades of experience fielding autonomous ground-based EMP sensors. Our system will exploit a signal-of-opportunity: persistent radar pulses from the SuperDARN radar in Kodiak, AK. Our plan is to deploy two bistatic stations around 100 km from HAARP in the direction of SuperDARN. Each station will consist of 31 antennas. Challenges to the design and operation of this system include: (i) difficulty in achieving high gain with low-profile antennas at SuperDARN HF frequencies, (ii) contending with SuperDARN's frequency variability (300 kHz short-term; 10-14 MHz long-term) that requires us to design a broadband-capable system, and (iii) the closely related issue of down-converting our 31 channel data for efficient local storage. This summarizes our solutions to these challenges and our plans for testing and deployment.

High Latitude Structure & Irregularities

High frequency surface wave oceanographic research radars as bistatic single frequency oblique ionospheric sounders and day-to-day ionospheric variability

Kaepler, Stephen *Clemson University*

Miller, Ethan (STR)

Markowski, Danielle (Clemson University)

Coleman, Lawrence (Clemson University)

We demonstrate that bistatic reception of high frequency oceanographic radars can be used as single frequency oblique ionospheric sounders. We develop methods that are agnostic of the software defined radio system to estimate the group range from the bistatic observations. The group range observations are used to estimate the virtual height and equivalent vertical frequency at the midpoint of the oblique propagation path. Uncertainty estimates of the virtual height and equivalent vertical frequency are presented. We apply this analysis to observations collected from two experiments, run at two locations in different years, but utilizing similar software defined radio data collection systems. In the first experiment, 10 days of data were collected in March 2016 at a site located in Maryland, USA, while the second experiment collected 20 days of data in October 2020 at a site located in South Carolina, USA. In both experiments, three Coastal Oceanographic Dynamics and Applications Radars (CODARs) located along the Virginia and North Carolina coast of the US were bistatically observed at 4.53718 MHz. The virtual height and equivalent virtual frequency were estimated in both experiments and compared with contemporaneous observations from a vertical incident Digisonde ionosonde at Wallops Island, VA, USA. We find good agreement between the oblique CODAR derived and WP937 Digisonde virtual heights. Variations in the virtual height from the CODAR observations and the Digisonde are found to be nearly in phase with each other. We conclude from this investigation that observations of oceanographic radar can be used as single frequency oblique incidence sounders. We show initial results of day-to-day bottomside variability using reception from multiple east-coast CODAR transmitters for the years 2020, 2021, and 2022. Day-to-Day, monthly, and yearly trends are shown.

HF Modeling, TIDs and Geolocation, HF Propagation & Systems

Generation of Realizations of Electron Density for Numerical Electromagnetic Propagation Simulations

Knepp, Dennis *NorthWest Research Associates, Inc*

Sotnikov, Vladimir

Numerical calculations of electromagnetic wave propagation that solve the parabolic wave equation generally require that the propagation medium consist of a number of phase-changing screens. In general, the screens can be random, deterministic, or a combination. Deterministic shapes include Gaussian lenses, elongated Gaussian striations, and more complicated shapes. Statistically-based or random phase screens are usually generated using Fourier transform techniques where the phase of the screen is calculated as the FFT of the product of the square root of the desired power spectrum and white Gaussian noise. Although it is easy to show that these statistically-generated realizations have the desired PSD and autocorrelation function, the technique to generate them is more mathematical than physics-based. In this paper we consider two physically intuitive techniques to generate random realizations of phase-screens.

Consider the two-dimensional problem, where the ionospheric structure is infinitely elongated in the y-direction. Let the z-direction be the direction of EM signal propagation. This geometry represents propagation in the equatorial region of the earth where the magnetic field lines are elongated in the north-south direction. We assume that the ionization consists of a finite number of Gaussians with random locations in the x-z plane and with random radii. The size of each Gaussian is drawn from a user-chosen probability density function. This simple description is sufficient to allow us to generate numerical realizations of the disturbed 2D ionosphere. Furthermore, for this situation of Gaussians, we can analytically calculate the PSD of electron density fluctuations and the PSD and autocorrelation function of the phase of the phase-screens used to represent the ionosphere. This enables the comparison of the PSD of the numerical phase-screens to the analytic PSD calculated for a very large number of phase screens.

We show several examples of realizations of ionospheric structure calculated using Gaussians as the basic, underlying striation. Two different probability density functions for the striation size distribution are calculated and we calculate the resulting PSDs of electron density fluctuations for the case that there are a large number of striations. One yields a power-law of the form usually observed in the ionosphere. The other leads to a power-law form of the correlation function of in-situ ionospheric structure. The latter form is useful in conceptual studies.

We also consider the use of infinitely elongated vortex structures created by a flow with velocity shear. For these examples, the ionospheric region consists of a large number of similar flux-vortices that are randomly located within a fixed volume, filling the volume with non-overlapping structure. The collection of vortices can be directly converted to phase-screens through numerical integration. The PSD of the phase of the phase-screens can also be estimated numerically and used to generate statistically based realizations that give similar propagation results.

Scintillation & Propagation Effects on GNSS and Other Systems

Using GNSS instantaneous phase differential to geolocate acoustic sources from August 2022 bolide

Lay, Erin Los Alamos National Laboratory

Tippmann, Jeff

Shao, Xuan-Min

Haaser, Robert

The ubiquity of GNSS receivers world-wide has led to many advances in ionospheric monitoring fairly inexpensively, and on a global scale. In this talk, we demonstrate the application of an instantaneous phase differential technique to geolocation acoustic wave sources in the ionosphere using high-rate (1-second cadence) ground-based GNSS measurements. We have applied the technique to the bolide that exploded over Northern Utah on 13 August 2022. The technique locates a path of the acoustic wave perturbations that is consistent with observations on the ground. We also discuss the limitations we discovered in the application of the technique to this bolide case.

HF Modeling, TIDs and Geolocation

Ionospheric Effects of Geospace Storm 5-6 August 2019

Luo, Yiyang V. N. Karazin Kharkiv National University

Chernogor, Leonid (V. N. Karazin Kharkiv National University)

Garmash, Konstantin (V. N. Karazin Kharkiv National University)

Guo, Qiang (Harbin Engineering University)

Zheng, Yu (Qingdao University)

The urgency of this work lies in the complex and synergistic nature of geospace storms, which involve interactions between magnetic, ionospheric, and atmospheric storms in the magnetospheric, ionospheric, and atmospheric environments. Since no two geospace storms behave exactly alike, it is crucial to study the effects of each new storm in order to reveal both the general laws and individual characteristics of storm processes. The purpose of this paper is to present general information about geospace storms and to analyze the features of magnetic and ionospheric storms. To analyze the magnetic environment, we used measurement results of magnetic field fluctuations in the range of 1 s to 1000 s from the Magnetometric Observatory of V. N. Karazin Kharkiv National University, as well as variations of the three components of the geomagnetic field from the Low-frequency observatory of the IRA NASU. To analyze the ionospheric environment, we used multi-frequency multi-path measurements performed at Harbin Engineering University (China), as well as ionosonde data. The main results of this work are as follows. An increase in the main parameters of the solar wind on August 5, 2019, led to a geospace storm that was mainly observed on August 5 and 6, 2019. The main phase of the magnetic storm occurred from UT 06:00 a.m. to UT 08:30 a.m. on August 5, 2019, while the recovery phase lasted at least 4 days. The magnetic storm exhibited significant variations in all components of the geomagnetic field, with an order of magnitude increase in oscillation levels of the geomagnetic field in the range of 400 s to 950 s. During the ionospheric storm, significant disturbances occurred in the F region of the ionosphere, while the E region of the ionosphere remained weakly perturbed. The ionospheric storm also severely affected the Doppler spectra of radio waves in the 5–10 MHz frequency range, with significant broadening of the spectra and quasi-periodic changes in the Doppler frequency shift with a period of 20–40 minutes and a duration of 120–240 minutes. The quasi-periodic variations in the Doppler frequency shift were due to quasi-periodic variations in the electron concentration, with the amplitude of their relative perturbations varying from 3% to 16%. On one of these paths, the amplitude of the Doppler frequency shift reached 0.7 Hz, while the amplitude of the relative perturbations of the electron concentration could reach 10–20%. Additionally, the ionospheric storm had little effect on the signal amplitude on most radio paths.

HF Modeling, TIDs and Geolocation, Space Weather Applications & Services, Storm Effects, HF Propagation & Systems

Ionospheric Effects During Moderate Earthquake in Japan on September 5, 2018

Luo, Yiyang V. N. Karazin Kharkiv National University

Chernogor, Leonid (V. N. Karazin Kharkiv National University)

Garmash, Konstantin (V. N. Karazin Kharkiv National University)

Guo, Qiang (Harbin Engineering University)

Shulga, Sergey (V. N. Karazin Kharkiv National University)

Zheng, Yu (Qingdao University)

The Earth's interior layers, atmosphere, ionosphere, and magnetosphere (EAIM) constitute an interconnected system that is open, dynamic, and nonlinear. The direct and reverse, positive and negative linkages among the subsystems within the EAIM system remain inadequately explored. A high-power release of energy from one of the subsystems can trigger interactions among the subsystems. In this study, we consider a moderate earthquake of Richter magnitude $M \approx 6.6$ as such a source. The objective of this paper is to describe time-varying characteristics of the HF radio waves observed along radio propagation paths over the People's Republic of China during the earthquake that occurred on September 5, 2018, in Japan. To observe the temporal variations in the characteristics of radio waves, a multi-frequency, multiple-path coherent radio system at Harbin Engineering University was used. Broadcasting stations located in the People's Republic of China, South Korea, Japan, Russia, and Mongolia were used as transmitters. The time variations in the Doppler spectra, the Doppler shift of the main mode frequency, and signal amplitudes were subjected to analysis. The measurements were carried out in the frequency range of 5 – 10 MHz over 14 radio propagation paths extending from 900 km to 1800 km with various orientations. The Doppler spectra were calculated in 7.5-second steps, with a root-mean-square Doppler line error of 0.02 Hz. The response of the ionosphere to a moderate earthquake were observed and analyzed. The delay time of the assumed response and the apparent speed of propagation of the disturbances were estimated. Our findings demonstrate that the seismic shock was followed by the spreading of Doppler spectra, and the Doppler frequency shift of the main mode varying with time in a quasi-periodic manner with an approximate period of 3 minutes for infrasound and 20-30 minutes for atmospheric gravity waves.

HF Modeling, TIDs and Geolocation, Space Weather Applications & Services, HF Propagation & Systems

Latest Developments on JPL's Global Ionospheric Mapping Software Suite: Multi-GNSS Support, High-Cadence, Near-Real-Time, and Error Quantification

Martire, Léo Jet Propulsion Laboratory (California Institute of Technology)

Green, Donald W., Jet Propulsion Laboratory (California Institute of Technology),

Ijima, Byron A., Jet Propulsion Laboratory (California Institute of Technology),

Komjáthy, Attila, Jet Propulsion Laboratory (California Institute of Technology),

Krishnamoorthy, Siddharth, Jet Propulsion Laboratory (California Institute of Technology),

Mannucci, Anthony J., Jet Propulsion Laboratory (California Institute of Technology),

Meng, Xing, Jet Propulsion Laboratory (California Institute of Technology),

Moore, Angelyn W., Jet Propulsion Laboratory (California Institute of Technology),

Runge, Tom F., Jet Propulsion Laboratory (California Institute of Technology),

Vergados, Panagiotis, Jet Propulsion Laboratory (California Institute of Technology),

Verkhoglyadova, Olga P., Jet Propulsion Laboratory (California Institute of Technology),

Mapping total electron content (TEC) of the ionosphere plays a critical role in a wide variety of services and products (Coster & Komjáthy, 2008). Numerous civilian applications of GNSS make extensive uses of high-precision point positioning (such as rail, highway, air, and sea traffic and navigation; search and rescue operations; and emergency responses). The precise computation of ionospheric calibrations, chiefly through various Global Ionospheric Maps (GIMs), enables high-accuracy point positioning, and mitigation of errors in the process. The very same ionospheric calibrations also enable systems such as NASA's Deep Space Network to perform reliable spacecraft tracking and navigation for planetary and interplanetary exploration.

Our focuses on the JPL Global Ionospheric Mapping (GIM) software suite developed at NASA's Jet Propulsion Laboratory (Mannucci et al., 1998). The approach is based on interpolating multi-GNSS high-rate TEC and the ionosphere is modeled as a set of one or more spherical shells, using specially designed basis functions estimating parameters in a Kalman filter approach. We review the main methods implemented in our software: acquisition of data, forming observables, setting up shell models, bias estimation, Kalman filtering, and outlier detection.

More importantly, we focus on new features implemented in the past few years. We describe the intricacies of adding the capability of using multi-GNSS observations (GPS, Galileo, GLONASS, and BDS). We highlight JPL-GIM's new capability to run in high-cadence mode, enabling ongoing real-time operations. We describe a case study of uncertainty quantification for our JPL-GIM model. We provide an update on our study of the 2022 Tonga event, showcasing a high-cadence multi-GNSS modeling capability that accurately resolves the ionospheric depletion following the eruption. We highlight samples of our validation cases, especially applied to the

new features. In conclusion, we provide an overview of our JPL ionospheric products, their parameters, as well as the current and futures uses.

Coster & Komjathy, 2008, Space Weather and the Global Positioning System, Space Weather 6, <https://doi.org/10.1029/2008SW000400>.

Mannucci et al., 1998. A global mapping technique for GPS-derived ionospheric total electron content measurements, Radio Science 33:565-582, <https://doi.org/10.1029/97RS02707>.

Space Weather Applications & Services

Revisiting refractive contribution to radio wave scintillation for polar cap applications

Nikoukar, Romina Johns Hopkins University Applied Physics Laboratory

Lamarche, Leslie, SRI International

Bals, Anna-Marie, Embry-Riddle Aeronautical University

Deshpande, Kshitija, Embry-Riddle Aeronautical University

Radio wave scintillation, rapid fluctuations in amplitude and phase of radio signals, is a major space weather hazard that hinders radio communication and global navigation satellite systems (GNSS). Although it is well-known that both diffractive and refractive effects contribute to scintillation, critical questions remain regarding their relative contribution to scintillation and the underlying ionosphere structure. Typically, the refractive contribution is thought to be slow-varying and associated with frequencies less than 0.1 Hz. This assumption, however, is not valid for polar cap measurements where ionosphere drift velocities are high. Based on the work of McCaffrey and Jayachandran [2019], which showed the refractive nature of high-frequency variations, we propose a new adaptive cut-off frequency determination technique for the high-rate data from CHAIN GNSS receivers, based on the Resolute Bay incoherent scatter radar (RISR) drift velocity measurements. With an improved cut-off frequency, we will have the ability to better isolate the refractive component of the scintillation, and as such to gain a better understanding of the underlying ionosphere structure, and the cascading of large-scale features (larger than Fresnel scale) to small-scale structures causing amplitude (diffractive) scintillation.

Scintillation & Propagation Effects on GNSS and Other Systems

Responses of the Nigerian low-latitude ionosphere to geomagnetic storms of the ascending and maximum phases of solar cycle 24

*Oyeyemi, E.O.*¹, A.O. Akala¹, D. Okoh, O.O. Odeyemi¹, B. Olugbon¹, P.O. Amaechi¹, O. J. Oyedokun¹, O.R. Idolor¹

¹Department of Physics, University of Lagos, Akoka, Yaba, Lagos, Nigeria

This study investigates the responses of the Nigerian ionosphere to thirteen geomagnetic storms that occurred during the ascending and maximum phases of the solar cycle 24. The Total Electron Content (TEC) data obtained from the Nigerian Global Navigation Satellite System (GNSS) network (NIGNET) were used for this study. The ionosphere over Nigeria recorded marked TEC variations around 1100–1700 LT with the highest values between 1400 LT and 1600 LT, and a minimum diurnal variation at 0600 LT. Another cogent piece of information from this study is that the values of TEC at all the five GNSS stations under investigation consistently matched one another. The implication of this is that the values of TEC, at both quiet time and storm time, at any location in Nigeria could be used as the representative values at any other locations in the country, particularly in areas where there are no GNSS systems. The equinoctial maxima and June solstice minima effects were clearly observed in our data. Furthermore, ionospheric irregularities occurrences also followed semiannual patterns with two peaks in April and October, and the least occurrences in June, and generally localized around 2000–0100 LT. At daytime during geomagnetic storms in the equatorial/low-latitude regions, the Prompt Penetration Electric Field (PPEF) is triggered to intensify a forward plasma fountain effect, while at nighttime, the reversed plasma fountain effect returns plasma backward to cause the Equatorial Ionization Anomaly (EIA) crests to contract, or totally coalesce the EIA structure to form a single strip of plasma density around the equator.

Keywords: GNSS; Geomagnetic storm; TEC; ionospheric irregularities; EIA

Changes in Polarization State of Transionospheric Radio Waves Driven by Difference in O- and X-mode Powers

Pandey, Kuldeep *University of Saskatchewan*

Kalafatoglu Eyiguler, E. Ceren (University of Saskatchewan)

Danskin, Donald W. (University of Saskatchewan)

Gillies, Robert G. (University of Calgary)

Yau, Andrew W. (University of Calgary)

Hussey, Glenn C. (University of Saskatchewan)

The Radio Receiver Instrument (RRI) of the Swarm-E/e-POP satellite can determine the polarization state of transionospheric radio waves. Coordinated experiments between ground transmitters and RRI show that the radio wave ellipticity oscillates from linear to circular when observed poleward of the transmitters. The RRI observations showed circularly polarized waves farther away from transverse propagation than expected from the theory. For radio waves with similar powers in the O- and X-modes, the circularly polarized waves are expected for transverse propagation (aspect angle 90°). However, the X-mode power was found to dominate over the O-mode at low elevations to the north of transmitter. A comparison is made between measurements from RRI of HF radio waves from the Saskatoon SuperDARN and a model that calculates the relative strength of X-mode over O-mode. The results show that the dominance of X-mode at select elevation angles can significantly change the ellipticity of the radio waves.

HF Modeling, TIDs and Geolocation

A study of the relative dynamics of ionospheric irregularities and GPS satellites on receiver tracking performance from a low-latitude station in the Indian longitudes

Paul, Ashik Institute of Radio Physics and Electronics, University of Calcutta

Biswas, Trisani (Institute of Radio Physics and Electronics, University of Calcutta)

Dynamics of the low-latitude ionospheric irregularities can make transionospheric satellite communication and navigation links vulnerable to medium introduced signal perturbation, sometimes to the extent of complete signal outage. Characteristics of the motion of satellites can introduce an additional metric on signal perturbation in relation to the drifting irregularity structures. This paper reports the relative contribution of GPS satellite geometry vis-à-vis irregularity movement on tracking loop performance of ground-based receivers during periods of ionospheric scintillations, observed from station Calcutta (22.58°N, 88.38°E geographic; magnetic dip 34.54°), located near the northern crest of Equatorial Ionization Anomaly (EIA). For this study, data recorded during three different solar activity periods (March 2014, March 2015 and March 2022) have been used to understand the correlation of east-west component of satellite velocity at Ionospheric Pierce Point (IPP) with the duration of loss-of-lock and rate of signal fading (<-10dB) noted from ground scintillation pattern observations. Results of this study show ~75-78% correlation between duration of loss-of-lock and eastward component of satellite velocity for all three period of observation. Duration of loss-of-lock has been observed to be shorter corresponding to westward satellite velocity. Signal fading rate is found to decrease with increasing satellite velocity, having median value of the fading rate cumulative distribution corresponding to satellite velocity of 16.69m/s, 31.76m/s and 19.14m/s respectively during March 2014, March 2015 and March 2022. Results of this study also indicate direction and component of satellite velocity at IPP to be a dominant cause of signal outage, even during periods of weak to moderate scintillations in the low latitudes.

Scintillation & Propagation Effects on GNSS and Other Systems, Equatorial Irregularities

Automatic real-time tool for processing of oblique sounding data

Paznukhov, D., K. Kraemer, T. Beach, B. Drummond, M. Proctor, K. Groves

Boston College, Institute for Scientific Research, 140 Commonwealth Ave., Chestnut Hill, MA 02467

Dao, Eugene (AFRL)

We present a robust, flexible system for real-time automated oblique ionogram data trace extraction and electron density profile (EDP) parameter estimation managed with quality control and data filtering capabilities. The developed system, named Optimal Approach System for Ionogram Scaling (OASIS) performs an automatic extraction of oblique traces; infers the ionospheric profile parameters and assesses data quality, parameter uncertainty and confidence. A novel approach used in this work was application of modern optimization algorithms to implement automatic ionogram processing. The ionospheric parameters are extracted by minimizing the difference between the real ionogram measurements and the ones modeled with specific ionospheric characteristics. The uncertainties of the extracted parameters are estimated based on the goodness of the fit evaluation and application of the Kalman Filtering technique. The calculated Quality Metrics consisting of Quality Flags (Accepted, Rejected, Flagged) and numerical uncertainty values for EDP parameters. A number of verification and validation tests have been performed. The first validation was made by processing of oblique sounding data and comparing them with vertical ionograms at the midpoint of the oblique propagations path. Second validation was processing oblique data and comparing with RIPE data-assimilative model results at midpoints of the oblique propagations path. Finally, the validation was performed by comparison of the measured and modeled oblique ionograms which were calculated using the ionosphere specification made by RIPE driven by a large amount of oblique sounding data processed with OASIS. We present analysis of the validation results and suggest the ways to further improve the performance of OASIS.

The views expressed are those of the authors and do not reflect the official guidance or position of the United States Government, the Department of Defense or of the United States Air Force.

Approved for public release; distribution is unlimited.

HF Propagation & Systems

Monitoring High-Latitude HF Absorption using Space-Based Lightning Measurements

Peterson, Michael LANL

Jeffery, Christopher

Geomagnetic storms affect radio propagation in bands used for critical radio communications at high latitudes. While NOAA provides operational data on HF absorption, this product only predicts disruptions from high-energy protons and not auroral electrons. We present modeling and observational analyses that support a novel concept for detecting all types of HF disruptions: directly measuring changes in the HF/VHF power spectra of serendipitous broadband lightning signals using space-based RF receivers.

We discuss a handful of intriguing high-latitude cases in the broadband EMP data collected by the Fast On-orbit Recording of Transient Events (FORTE) satellite during the April 1998 and July 2000 storms that show a distinct change in the lightning power spectra once each storm commences. Moreover, the lightning power spectral slope is correlated with enhancements in the GOES proton flux data over the course of the storm. However, these observations are limited because the RF payload was often changed from independently triggering on impulsive events (like lightning) to software-defined data collections at high latitudes to address other FORTE mission priorities.

Further study is needed to build robust statistics of lightning power spectral changes during geomagnetic storms and to quantify the effects of HF absorption in the recorded signals. We are currently exploring methods for automating the detection of significant power spectral changes in our on-orbit EMP data holdings in the hope of developing a future CubeSat mission.

High Latitude Structure & Irregularities

Detrending GOLD EUV Data to Reveal Equatorial Plasma Bubble Structures

Pradipta, Rezy Boston College, Institute for Scientific Research

Groves, Keith (Boston College)

Huang, Chaosong (AFRL)

We report our investigation on the detection and classification of equatorial plasma bubble (EPB) structures in the Global-scale Observations of the Limb and Disk (GOLD) EUV data. We have developed a novel technique for detrending the nighttime GOLD EUV irradiance data, which helps reveal large-scale field-aligned depletions associated with EPBs. The data detrending technique is a two-dimensional generalization of the rolling-barrel data detrending technique [Pradipta et al., 2015] that operates in one dimension. In this case, the rolling barrel is replaced with a rolling ball with two degrees of freedom to navigate across a two-dimensional uneven terrain defined by the nighttime GOLD EUV irradiance data. The inferred baseline irradiance and the detrended irradiance data are subsequently transformed into geomagnetic coordinate in order to trace the position of the equatorial ionization anomaly (EIA) crests and the shape of EPB depletions. In the data analysis, the detected EPB depletions may appear either straight or curved with an inverse-C shape, depending on the solar local time. Zonal drift velocities of the detected EPBs are deduced based on sequential frames of GOLD EUV observation data. Afterwards, the computed EIA and EPB traces are transformed back from geomagnetic into geographic coordinate for realistic comparison with the original GOLD EUV observation data.

Equatorial Irregularities, Optical Remote Sensing

Identifying and Attributing Signal Distortions Using Machine Learning Techniques

Proctor, Matthew Institute for Scientific Research, Boston College

Rino, Charles (Boston College)

Groves, Keith (Boston College)

Paznukhov, Dima (Boston College)

Smith, Dallin (Air Force Research Laboratory)

Radio ionospheric scintillation can result in severely degraded signal performance of navigation systems such as the Global Positioning System (GPS) and global communication systems such as UHF SATCOM. Plasma instability processes in the ionosphere can cause structures (depletions and/or augmentations from the ambient electron density) called ionospheric irregularities or plasma bubbles, which can range in scale size from 10 km to decimeters. As electromagnetic waves traverse these irregularities, they experience scattering, diffraction, and/or fluctuations in the signal's amplitude and phase, effects referred to as ionospheric scintillation. These consequences depend in part on the transmitted source frequency, the density of ionospheric plasma, the strength and spectral characteristics of the irregularities, and numerous other characteristics. Multipath error results from interference between two radio waves which have travelled paths of different lengths usually reflected or diffracted from local objects. Awareness of any Radio Frequency Interference (RFI) on satellite communication is of paramount concern for global radio users. When RFI is present, knowing the source of the interference is extremely valuable to an end user. Using machine learning techniques, a model is being developed to distinguish between ionospheric scintillation, local interference, and multipath. The model has demonstrated great effectiveness in distinguishing between these classifications.

The views expressed are those of the authors and do not reflect the official guidance or position of the United States Government, the Department of Defense or of the United States Air Force.

Approved for public release; distribution is unlimited.

Applications of Machine Learning to Ionospheric Science and Engineering

Applications of a Novel Modular High Frequency Measurement Platform in Ionospheric Observation

Reuschel, Torsten *University of New Brunswick*

Kashcheyev, Anton (University of New Brunswick)

Trottier, Philippe (University of New Brunswick)

Jayachandran, Thayyil (University of New Brunswick)

Monitoring the space weather environment is crucial to understanding the upper atmosphere dynamics. In particular, the prediction of dynamic ionosphere characteristics is required for mitigating their detrimental impact on the operation of satellite-based navigation and communication systems. Ionosondes are well-established instruments to gain insight into the state of the ionosphere. For example, a mono-static ionosonde, also known as vertical ionospheric sounder, may transmit in the frequency range from 1 to 30 MHz. The vertically incident waves are reflected from different layers of the ionosphere, and are received and processed by the instrument to reconstruct a corresponding electron density profile.

Established ionosonde systems such as the Canadian Advanced Digital Ionosonde have been in operation for decades. However, today's research demands for flexibility with regard to operating modes and observation conditions. This contribution makes use of a novel modular measurement platform that aims to meet this need based on affordable digital hardware and software defined radio. We present application examples and practical experience from working with the newly developed platform from the perspective of academia. A particular focus is placed on operation modes of the platform such as broadband receiver, riometer, and ionosonde. However, further modes of operation such as plasma drift measurements or over-the-horizon radar can be seamlessly and concurrently integrated. The analysis is performed with regard to different signal input conditions, including different local times, seasons, and geomagnetic conditions.

HF Propagation & Systems

Sferic-based tomography for D-region imaging

Richardson, David *Georgia Institute of Technology*

*Cohen, Morris (Georgia Institute of Technology, mcohen@gatech.edu)

The lower ionosphere, in particular the D region (60-90 km), is difficult to reach with direct measurements (balloons, satellites, etc.) due to its altitude range. Instead, researchers have relied on very low frequency (VLF, 3-30 kHz) and low frequency (LF, 30-300 kHz) remote sensing techniques. Using these techniques, D-region ionosphere models have historically estimated electron density along transmitter-to-receiver paths, in particular path-averaged electron density. While these techniques do provide useful geophysical information, they are somewhat lacking in terms of spatial information. Our work utilizes recent improvements in lightning-based path-average estimates in combination with tomography to produce 3D maps of electron density within the D-region ionosphere. During quiet time, we are able to produce daytime, nighttime, and day-night terminator electron density maps within our area of confidence (Gulf of Mexico and SE United States). Based on our results in the synthetic case, we estimate our error to be less than 10% within this region. During the 2017 solar eclipse, we also show strong agreement between our modeled electron density and the eclipse location demonstrating our model's ability to capture interesting geophysical phenomena. As this technique is developed further, it is our hope to include information from VLF transmitters into the model to unify existing lightning-based and transmitter-based methods. Initial results in this direction indicate the inclusion of VLF transmitters increases the area of confidence to include more northern regions of the United States.

*Presenting author

HF Propagation & Systems, Applications of Machine Learning to Ionospheric Science and Engineering, D-Region Ionosphere

Forward Propagation Geometrical Optics and Beam Steering

Rino, Charles^{*(1)}, Charles Carrano⁽¹⁾, and Keith Groves⁽¹⁾

(1) Institute for Scientific Research, Boston College, Chesnut Hill, MA, USA

1 Introduction

The propagation of electromagnetic (EM) waves is governed by Maxwell's equations. Constitutive relations characterize the interaction of the electric and magnetic field with the medium. For the earth's ionosphere and atmosphere the constitutive relation is a frequency-dependent tensor or scalar. Vector wave equation follows from the time-harmonic form of Maxwell's equations upon neglecting the gradient of the electric-field divergence. For the purposes of this paper we consider the scalar form of the wave equation, which we write here in two forms:

$$\nabla^2 \psi(x; \eta) + k^2 \psi(x; \eta) = -k^2 X(x; \eta) \psi(x; \eta) \quad (1)$$

$$\left[\frac{\partial^2}{\partial x^2} + \nabla_{\perp}^2 + k^2 K(x; \eta) \right] \psi(x; \eta) = 0 \quad (2)$$

where $K(x; \eta) = \sqrt{n(\mathbf{r})} = 1 + X(x; \eta)$ In the first form of the wave equation the term involving $X(x; \eta)$ acts as an induced source. The second form incorporates $X(x; \eta)$ within an operator that acts on the total field. The weak-scatter theory and the theory of propagation in stochastic media proceed from the first form of the wave equation. The multiple phase screen (MPS) method is often thought of as a guiding principle embodied in the forward propagation equation (FPE):

$$\frac{\partial \psi(x, \eta)}{\partial x} = \Theta \psi(x, \eta) - ikX(x, \eta)/2 \psi(x, \eta), \quad (3)$$

where $\Theta \psi(x, \eta)$ is the free-space propagation operator.

In two recently published papers, [1] and [2], we extended the FPE to accommodate vector HF propagation, with encouraging results. However, as noted in the second paper, a disparity between vector forward propagation realizations and geometrical optics predictions was found. The disparity is the result of a fundamental constraint which limits *standard* MPS methods to narrow-angle propagation. The limitation is well known in acoustic propagation where wide-angle extension of the narrow-angle scatter theory are used routinely. The HF applications will be discussed in a separate presentation. The remainder of this paper will discuss extensions of geometrical optics as a diagnostic intermediary.

For scalar fields geometric optics ray theory takes a particularly simple form:

$$\frac{d^2 \mathbf{r}}{ds^2} + \frac{dn}{nds} \frac{d\mathbf{r}}{ds} = \frac{\nabla n}{n}, \quad (4)$$

where s is the path distance. Our FPE ray theory comparisons used only the central path of a ray bundle. However, upon comparison of (3) and (4), a full-field theory effectively enhances the free-space operator to accommodate refraction. Figure 1 shows the optical path for a ray bundle launched from representative earth surface into a Chapman layer. Contours of constant optical path are phase fronts, which vary linearly in the propagation coordinate system, indicating beam steering. We review and demonstrate reconstruction of beam fields from ray optics.

References

- [1] C. Rino and C. Carrano. A vector theory for forward propagation in a structured ionosphere. *Journal of Atmospheric and Terrestrial Physics*, 2021. doi.org/10.1016/j.jastp.2021.105558.
- [2] C. Rino and C. Carrano. A vector theory for forward propagation in a structured ionosphere with a conducting boundary. *Journal of Atmospheric and Terrestrial Physics*, 223, 2021. doi.org/10.1016/j.jastp.2021.105740.

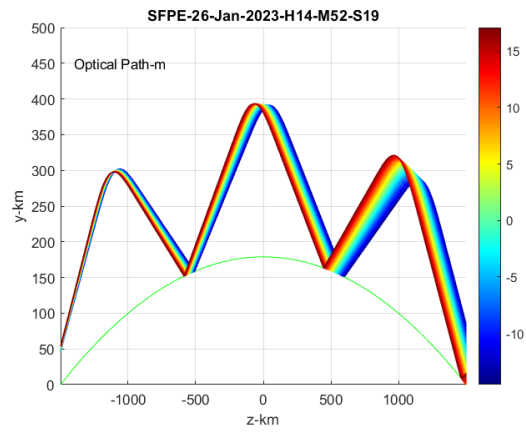


Figure 1. Display of 10 MHz optical path for a ray bundle launched from a curved earth surface into a Chapman layer.

New Utilities for Diagnostic Ionospheric Signal Processing

Rino, Charles^{*(1)}, Charles Carrano⁽¹⁾, Matthew Proctor⁽¹⁾, Dima Paznukhov⁽¹⁾, and Keith Groves⁽¹⁾

(1) Institute for Scientific Research, Boston College, Chesnut Hill, MA, USA

1 Introduction

Beacon satellite signal processing for ionosphere diagnostics starts with sampled intensity and phase (GPS) or differential phase (dual-frequency systems). Scintillation is a complex modulation imparted to the signal. The signal phase includes a Doppler-shift contribution due to changing range and a contribution proportional to the path-integrated electron density (TEC). Dual-frequency measurements are used to remove the geometric-Doppler contribution. The residual TEC contribution is slowly varying. TEC measurement can be degraded by scintillation, which varies more rapidly. The low-frequency content of intensity scintillation is suppressed by Fresnel filtering. However, signal intensity varies inversely with path length and directionally varying antenna patterns. The scintillation index, $S4 = \sqrt{(\langle I^2 \rangle / \langle I \rangle^2 - 1)}$, is a standard measure of scintillation intensity, which is biased by additive noise. Preprocessing operations are used to isolate scintillation and TEC. Noise bias correction is also desirable under low signal-to-noise (SNR) conditions.

Digital data processing operations can draw on a variety of digital data processing utilities, e. g. wavelets, adaptive filtering, and fast iterative filtering as well as conventional digital filtering. Detrending, as the name implies, uses an estimate of the average intensity to generate a signal with constant average intensity over a prescribed measurement interval. The detrending operation does not require digital filtering. However, it is often desirable to impose a low-pass frequency cutoff based on knowledge of imposed intensity variation scales. Similarly, because of the inverse power-law spectrum frequency dependence of phase scintillation, rms phase is determined by the high-pass filtering operation that isolates the scintillation content.

This paper will demonstrate a digital filter impulse response design that proceed directly from a specification of the frequency transfer function using only discrete Fourier transforms [Rino1971]. The result is more accurate than standard signal processing toolbox utilities, which use transformed continuous filter designs based on a second-order cascade approximation. Figure 1 shows a Butterworth filter example. Figure 2 shows an example of filtered phase scintillation under moderate scintillation conditions.

To the extent that detrending has isolated the intensity scintillation, the noise contribution remains. In an early paper by VanDirendonck [DKH93] estimates of wideband and narrow band signals were subtracted prior to intensity calculation. However, if noise contribution is additive, uncorrelated, and exponentially distributed the following model can be used directly:

$$SI = (S4^2 + 4/SNR^2 + 1/SNR^4)/(1 + 2/SNR^2 + 1/SNR^4). \quad (1)$$

Examples of direct correction of the noise bias will be demonstrated. Matlab code for both filter development and S4 correction will be made available.

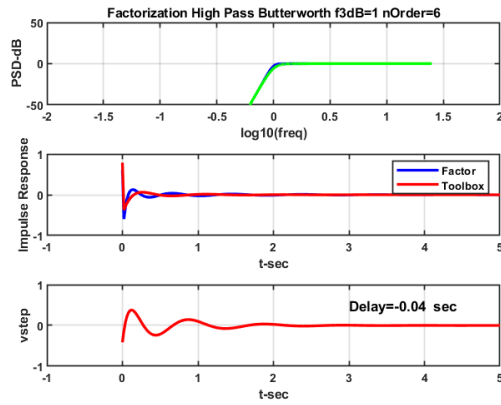


Figure 1. Top frame compares exact (blue) and toolbox (green) Butterworth filter. Middle frame shows transfer functions. Bottom frame shows step response for filter delay.

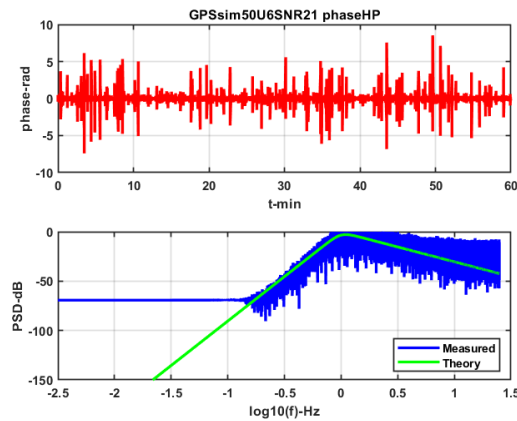


Figure 2. Top frame is filtered phase from simulated scintillation with $S_4 = 0.6$. Lower frame shows measured phase spectrum (blue) with defining phase-screen spectrum. High frequency phase enhancement is due to phase jumps.

References

- [DKH93] A. J. Van Dierendonck, J. Klobuchar, and Q. Hua. Ionospheric scintillation monitoring using commercial single frequency *c/a* code receivers. *Proc. ION ITM, Salt Lake City, UT*, (September), 1993.
- [Rino1971] C. Rino. Factorization of Spectra by Discrete Fourier Transforms *IEEE Transactions on Information Theory* 1971July 1970

Improving IRI's topside formulation for a better assimilation of GNSS TEC data during the local winter

Servan-Schreiber, Nina *Boston College ISR*

*Paznukhov, Dima

GNSS TEC measurements constitute a world-wide and readily available source of data for the study of the ionosphere. In recent years, there has been an increase in the combined use of GNSS TEC data and ionospheric climate models such as IRI to improve the estimation of Electron Density Profiles (EDP) parameters, which can only be measured by a sparse network of ground-based instruments around the globe. In this study, we use GNSS TEC measurements to derive EDP peak density parameter foF2 and to compare it to the IRI model prediction. We also investigate ways to improve the efficiency of using GNSS TEC measurements in concurrence with IRI by adjusting its topside profile NeQuick sub-model.

Slant TEC measurements are calibrated for a single GNSS receiver and converted to vertical TEC assuming a single layer approximation of the ionosphere. We minimize the difference between this measured TEC and the IRI-modeled TEC by varying an effective ionospheric parameter foF2 used to drive the IRI model. The resulting foF2 parameter estimate is therefore derived from GNSS TEC data used in concurrence with an ionospheric model. Using ten GNSS receivers co-located with ionosondes for ground-truth values, we compare the RMSE of the IRI-modeled foF2 with and without the use of GNSS TEC. The study spans years 2014 to 2020, which covers both high and low solar activity conditions. Our results show that (1) using GNSS TEC data in concurrence with IRI improves the estimation of foF2 to varying degrees depending on the latitude of the studied location, and (2) there is a persistent degradation of the results using GNSS TEC data during the local winter months, independent of the location or year of study. Based on recent studies of the behavior of the ionospheric slab thickness, we hypothesize that the degradation comes from a weakness in IRI's formulation of the topside ionosphere. Using an empirically-developed function as a diurnal scaling factor of the topside scale height, we show that it is possible to improve the efficiency of using GNSS TEC data in concurrence with IRI for the estimation of foF2 during the local winter.

Space Weather Applications & Services, Topside & Plasmasphere

*Presenting Author

Reviving High-Speed Releases using Sounding Rockets and the Space Measurements of A Rocket-Released Turbulence (SMART) Experiment

Siefring, Carl US Naval Research Laboratory, Plasma Physic Division

Ganguli, Gurudas

Gatling, George

Coombs, Joseph

Crabtree, Christopher

Fletcher, Alex

Amatucci, William

Netwall, Christopher

Falcone, Nicholas (Naval Surface Warfare Center)

Ferrell, William (NASA Goddard Space Flight Center)

Holzworth, Robert (University of Washington)

McCarthy, Michael (University of Washington)

Space Measurements of A Rocket-Released Turbulence (SMART) is a sounding rocket experiment to explore the role of the weak turbulence process known as nonlinear (NL) scattering in space plasmas. The experiment is modeled after similar high-speed Barium releases conducted since the mid-1970s that generated high-speed Barium (Ba) atoms using a shaped charge explosion. A fraction of Ba is atomized and ejected at velocities around 8 km/s. Such releases have been used to study multiple physical processes in the ionosphere. One example are Critical Ionization Velocity (CIV) experiments such as NASA CRIT II experiment flown in 1989. The technological expertise to generate such high-speed releases have largely been lost and in general they were not well documented. One of the goals of the SMART program is to revive this technology. In developing the SMART experiment, a number of issues concerning range safety have occurred, limiting available launch sites, trajectories, and times.

In SMART, the Ba atoms are fired perpendicular to the Earth's magnetic field in sunlight. The Ba atoms then photoionize forming an ion ring velocity distribution of heavy Ba⁺ that is unstable and known to generate LH turbulence. Theoretical analyses indicate that weak turbulence processes causes NL scattering of LH waves into whistler waves. Previous experimental Ba explosive releases measured large amplitude electric fields, indicate possible generation of electromagnetic waves and, in one case, resulted in energetic particle precipitation. However, none of these experiments had sufficient measurements to separate the EM contribution to the electric field and confirm NL scattering. For SMART, simultaneous measurements are made of electrostatic lower-hybrid (LH) waves in the ionosphere and the scattered electromagnetic (EM) waves (e.g., whistlers) with both the sounding rocket in the ionosphere and remotely with a satellite in the magnetosphere. The effect of Very Low Frequency whistler turbulence (e.g.,

lightning generated whistler waves) is of particular importance to the dynamics in the inner magnetosphere and the radiation belts, but also has more global relevance, e.g. in solar wind turbulence.

We will discuss the SMART experiment, progress in rediscovering the technology of creating high-speed Ba releases from sounding rockets, and some of the pit-falls that currently limit launching similar payloads.

This work was supported by Defense Advanced Research Projects Agency and the NRL Base Program

DISTRIBUTION STATEMENT A. Approved for public release. Distribution is unlimited.

Active Experiments

The Development of the Radio Frequency Ionospheric Scintillation Attribution (RISA) Tool

Smith, Dallin AFRL

Ronald Caton¹, Keith Groves², Theodore Beach², Charles Carrano², Alan Hoskinson², William McNeil², Donald Mizuno²

¹Air Force Research Laboratory, Ionospheric Impact Branch, Kirtland AFB, NM 87117

²Boston College, Institute for Scientific Research, Chestnut Hill, MA 02467

Scintillation occurs when radio waves traverse ionospheric plasma turbulence or irregularities and develop random fluctuations in amplitude, phase, and other signal properties. Scintillation negatively impacts systems with trans-ionospheric radio links such as satellite communications, PNT (position, navigation, and timing) systems and space-based radar, as well as ground-based surveillance systems. The irregularities are formed by plasma instabilities and affect radio propagation differently depending on the transmitted radio frequency. When scintillation disrupts systems, determining attribution—e.g., intentional jamming, equipment or environment is vital knowledge. The Radio Frequency (RF) Ionospheric Scintillation Analysis (RISA) tool addresses the ionospheric scintillation impacts for space domain awareness. It provides global specification and nowcast of the ionospheric scintillation environment using on-demand data driven projections and climatology. The current version of RISA software assimilates scintillation measurements from both ground-based geostationary beacons and GNSS receivers and space based GNSS radio-occultation measurements. By fusing these diverse data sources, the model provides 24/7 global scintillation coverage at low latitudes over land and sea. RISA ingests these observations to synthesize the best estimate of the plasma turbulence strength (CkL) of the ionosphere and generates a 3D data cube that supports consistent RF link analysis for arbitrary geometries, frequencies, and platform dynamics. The system is modular and the data cube contains only “weather” data (turbulence parameter), such that it can be easily separated and distributed apart from propagation effects or system products. Furthermore, the data are highly compressible as measurements from all sensors are mapped to a 1D equivalent value at the magnetic equator; thus, having only the 1D information and a small number of configuration parameters, a user can quickly regenerate the entire 3D scenario. The fusion algorithm is also readily scalable; future versions may include additional data sources, such as other RF links, in situ density observations, ground-based TEC fluctuations, and/or UV imagery. The model may also be extended to mid- and high latitudes without major technical challenges.

An overview of the model and its performance under a variety of conditions will be presented.

The views expressed are those of the authors and do not reflect the official guidance or position of the United States Government, the Department of Defense or of the United States Air Force.

Approved for public release; distribution is unlimited.

Space Weather Applications & Services; Scintillation & Propagation Effects on GNSS and Other Systems; HF Modeling, TIDS and Geolocation

Characterization of the Daytime Ionosphere with ICON EUV Airglow Limb Profiles

Stephan, Andrew *U.S. Naval Research Laboratory*

Sirk, Martin (University of California Berkeley)

Korpela, Eric (University of California Berkeley)

England, Scott (Virginia Polytechnic Institute and State University)

Immel, Thomas (University of California Berkeley)

The NASA Ionospheric Connection Explorer Extreme Ultraviolet spectrograph, ICON EUV, images one-dimensional altitude profiles of the daytime extreme-ultraviolet (EUV) airglow between 54-88 nm. This spectral range contains several OII emission features derived from the photoionization of atomic oxygen by solar EUV. The primary target of the ICON EUV is the bright OII (4P – 4S) triplet emission spanning 83.2-83.4 nm that is used in combination with a dimmer but complementary feature (2P – 2D) spanning 61.6-61.7 nm that are jointly analyzed with an algorithm that uses discrete inverse theory to optimize a forward model of these emissions to infer the best-fit solution of ionospheric O⁺ density profile between 150-450 km. From this result, the daytime ionospheric F-region peak electron density and height, NmF2 and hmF2 respectively, are inferred. The science goals of ICON require these measurements be made in the regions of interest with a vertical resolution in hmF2 of 20 km and a 20% precision in NmF2 within a 60-second integration corresponding to a 500 km sampling along the orbit track. This paper describes the results from the ICON EUV over the first year of the mission, which occurred primarily under solar minimum conditions.

Optical Remote Sensing

A “Prediction Model” for the Occurrence or No-occurrence of Density Irregularity in Space Constructed with the ROCSAT Data

Su, Shin-Yi National Central University, Taiwan

S.-Y. Su^{1,2}, H.-H. Ho^{2,3}, C.-K. Chao^{1,2}, L.-C. Tsai¹, and C. H. Liu⁴

1. Center for Space and Remote Sensing Research, National Central University, Chung-Li, Taiwan.
2. Department of Space Science and Engineering, National Central University, Chung-Li, Taiwan.
3. Central Weather Bureau, Taipei, Taiwan.
4. Academia Sinica, Taipei, Taiwan.

The density variations at a constant height such as observed by the circularly orbiting ROCSAT-1 spacecraft are studied to construct a “prediction model” for the occurrence or no-occurrence of an equatorial plasma bubble (EPB). This global prediction model is different from previous studies carried out at a local ground station by observing the variation of the ionospheric height and the occurrence of equatorial spread-F/EPB events. The model uses the density increment above the seasonal mean to predict the EPB occurrences. It does not merely provide the occurrence probability of EPB occurrences. Instead, the ROCSAT “prediction model” is to predict the occurrence or no-occurrence of the density irregularity/EPB along the ROCSAT orbit by constructing a contingency table to count the number of successes in predicting the EPB occurrences, failures in predicting the occurrences, and false alarms in a month. Different thresholds of density increment are used for the criteria in the prediction to obtain the optimal result in the prediction model. The optimal model for predicting the global irregularity/EPB occurrences varies between 75% and 85% for any season in 1999 to 2004.

Equatorial Irregularities

Estimation of Ionospheric Scintillation Index S4 from Rate of Change of Total Electron Content Index (ROTI) in Low Latitudes

Surco Espejo, Teddy Institute for Scientific Research/Boston College

Carrano, Charles (Institute for Scientific Research/Boston College)

Groves, Keith (Institute for Scientific Research/Boston College)

Beach, Theodore (Institute for Scientific Research/Boston College)

Ionospheric scintillations are fluctuations in the phase and amplitude of the signals from GNSS satellites occurring when they cross regions of electron density irregularities in the ionosphere and hence can cause significant errors in positioning based on Global Navigation Satellite System (GNSS). Scintillation is usually characterized by amplitude and phase scintillation index (S4 and $\sigma\phi$). However, the specialized receivers that can generate the scintillation indices are not available all around the world, which limits the application of these approaches. In spite of that, there are numerous inexpensive geodetic receivers that are capable of measuring the Total Electron Content (TEC) and Rate of TEC (ROTI). The ROTI is a commonly used measure of ionospheric irregularities level.

In order to overcome this problem, the relationship between ROTI and scintillation indices (S4 and $\sigma\phi$) has been studied. In the present work is applied a quantitative theoretical model developed for ROTI related to the phase structure function. This theoretical model is a scaled version of the structure function of phase fluctuations imparted to the wave by the irregularities and relates the statistical measures of TEC fluctuations and ionospheric irregularities of associated scintillations. The present model for ROTI accounts for the dependence on the sampling interval, satellite motion, propagation geometry and the spectral shape, strength, anisotropy and drift of ionospheric irregularities.

The focus of this work is to estimate the ROTI based on data from GNSS receivers located in low latitudes then, the S4 index is calculated using the relationship of ROTI/S4. Measured drifts will be used to estimate the effective scan velocity, when it is available. In this work we estimated the error comparing the S4 predictions with the S4 computed from 50 Hz intensity samples. In addition, this study evaluates the S4 index estimated using a climatological RISA model for drift, different sampling rates ($\delta t = 1$ s and $\delta t = 10$ s), GPS frequency (L1, L2C and L5).

Scintillation & Propagation Effects on GNSS and Other Systems, Equatorial Irregularities

Gradient drift instability and decameter ionospheric irregularities at the edge of polar holes

Thaller, Scott Orion Space Solutions

Hughes, Joe (Orion Space Solutions)

Crowley, Geoff (Orion Space Solutions)

Noto, John (Orion Space Solutions)

Blay, Ryan (Orion Space Solutions)

The polar and high latitude regions of the ionosphere are host to several complex plasma processes involving Magnetosphere-Ionosphere coupling, convection, auroral dynamics, and so on. The magnetic field lines from the polar cusp down through the auroral region map out to the magnetosphere and project the footprint of the large-scale convective process driven by the solar wind onto the ionosphere. This region is also a unique environment where the magnetic field is oriented vertically resulting in horizontal drifts along closed, localized, convection patterns, and where prolonged periods of darkness during the winter result in the absence of significant photoionization. This set of conditions results in unique ionospheric structures which can set the stage for the generation of ionospheric instabilities, such as the gradient drift instability (GDI), which gives rise to density irregularities that impact over-the-horizon radars and GPS signals. Thus, in addition to being a rich area for scientific research, the processes and phenomena that occur in the high latitude ionosphere are important for GPS/GNSS positioning, navigation, and timing (PNT), and for radar detection and ranging. One such resulting phenomenon, polar holes, are large, ~1000 km, ionospheric structures with a plasma density an order of magnitude lower than the typical background. Polar holes tend to form during polar winter during periods of low geomagnetic activity when the ionospheric convection proceeds slowly. The edge of the polar hole is a significant density gradient, and thus it should be possible that the GDI occurs there. If so, the resulting production of small-scale density irregularities will give rise to scintillation of GNSS signals and backscatter on HF radars. These effects have been observed on the steep gradients at the edge of polar patches, which are large localized enhancements of ionospheric plasma density.

In this study, we investigate whether these small irregularities can occur at the edges of polar holes. Specifically, we target the leading edge of the polar hole under ExB convective motion. At such a location, the ExB drift velocity is parallel to the density gradient, which is a condition conducive to the GDI growth. We use the Ionospheric Data Assimilation 4-Dimensional (IDA4D) and Assimilative Mapping of Ionospheric Electrodynamics (AMIE) models to characterize the high latitude ionospheric density and ExB drift convective structures, respectively, for nine polar hole events identified using RISR-N incoherent scatter radar. The combined IDA4D and AMIE assimilative outputs indicate where the GDI could be triggered, e.g., locations where the density gradient and ExB drift velocity have parallel components and the growth rate is smaller than the characteristic time over which the convective pattern changes, in this case, ~1/15 min. The presence of decameter ionospheric plasma irregularities is detected using the Super Dual Auroral Radar Network (SuperDARN) of HF coherent scatter radars. The

presence of ionospheric radar returns in regions conducive to GDI growth strongly suggest the GDI is producing decameter scale plasma irregularities. We will present evidence that the GDI at the edge of polar holes is associated with radar returns under suitable observing conditions. "

High Latitude Structure & Irregularities